Intensity and dynamics of extreme cold spells of the 21st century in France from CMIP6 data: Supplementary Material.

Camille Cadiou[1] and Pascal Yiou[1]

[1]Laboratoire des Sciences du Climat et de l'Environnement, UMR 8212 CEA-CNRS-UVSQ, IPSL and U Paris Saclay, 91191 Gif-sur-Yvette CEDEX, France

Correspondence: Camille Cadiou (camille.cadiou@lsce.ipsl.fr)

1   Introduction

This document contains the Z500 anomaly and standard deviation maps of the 10 CMIP6 models used with KACE-1-0-G for SWG simulations of extreme cold spells in the article *Intensity and dynamics of extreme cold spells of the 21st century in France from CMIP6 data*: BCC-CSM2-MR, CanESM5, CESM2-WACCM, CNRM-ESM2-1, EC-Earth3, FGOALS-g3, IPSL-CM6A-LR, MPI-ESM1-2-LR, MRI-ESM2-0 and NorESM2-LM.
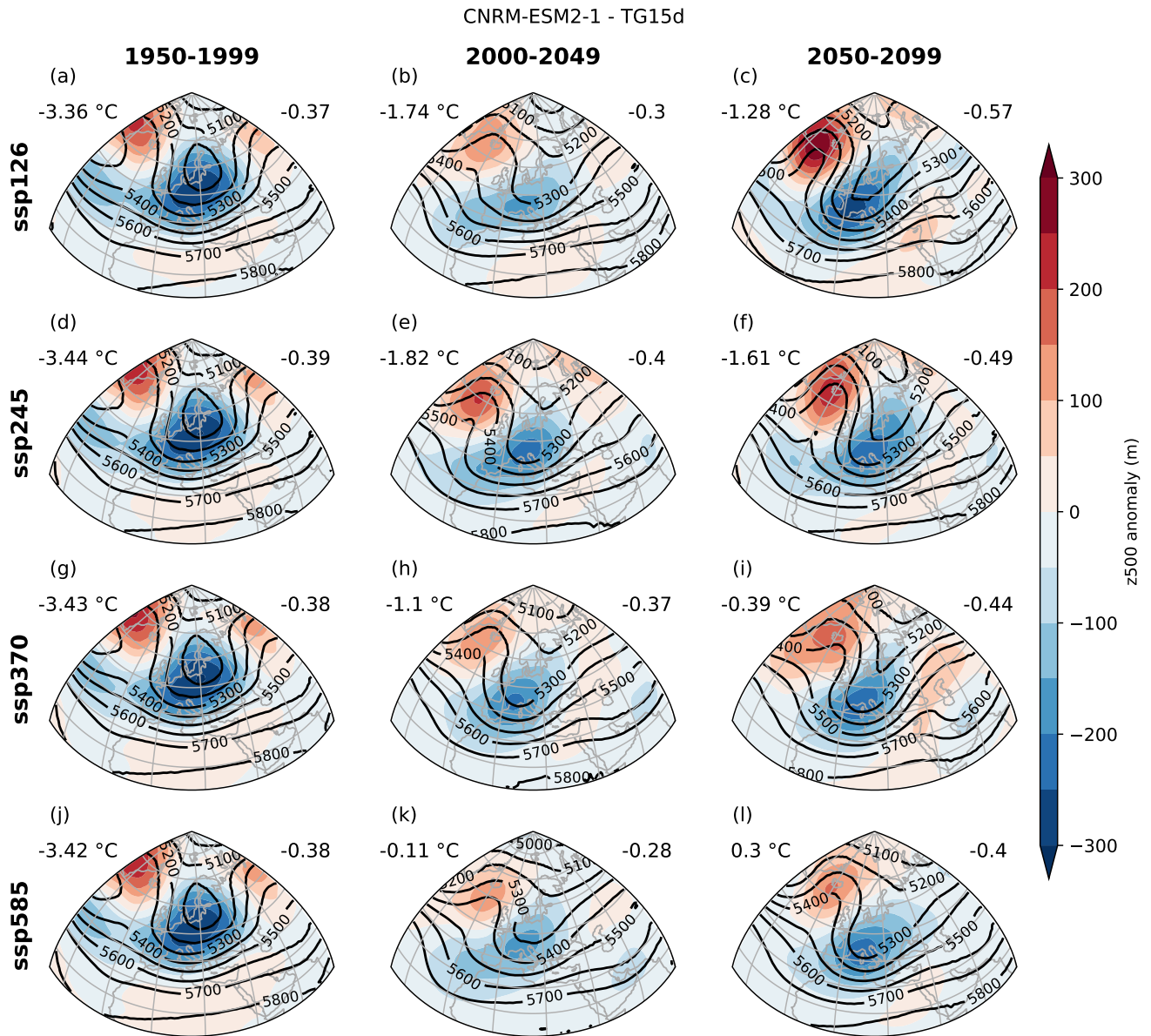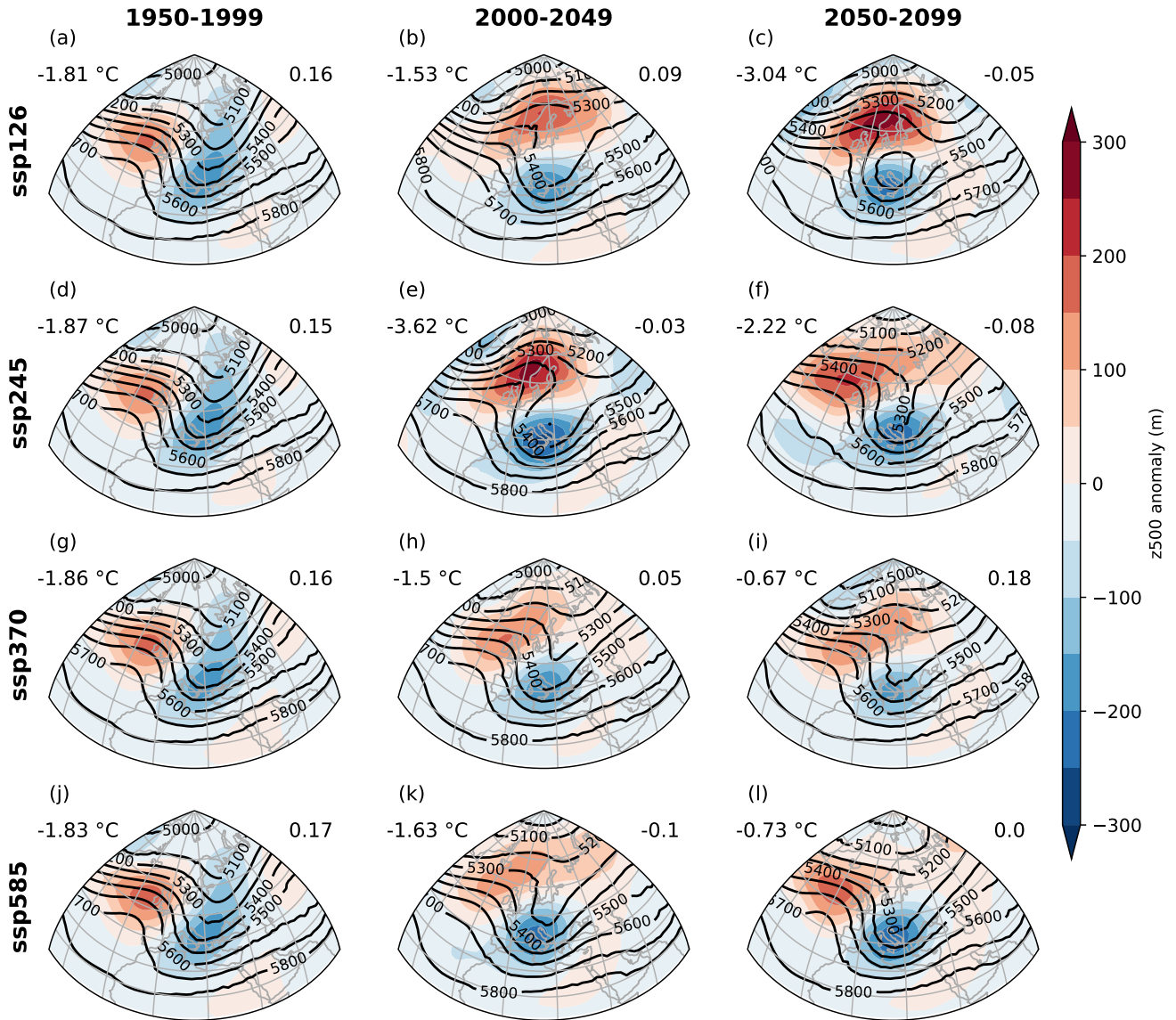
2   Z500 anomaly maps

Fig. S1. Absolute values (contours, in m) and anomalies (shaded areas, in m) with respect to 1950-1999 of 500-hPa geopotential height (Z500) for the 10% coldest SWG simulations (i.e. 100 trajectories) for each period (columns) and SSP (rows) in CNRM-ESM2-1.
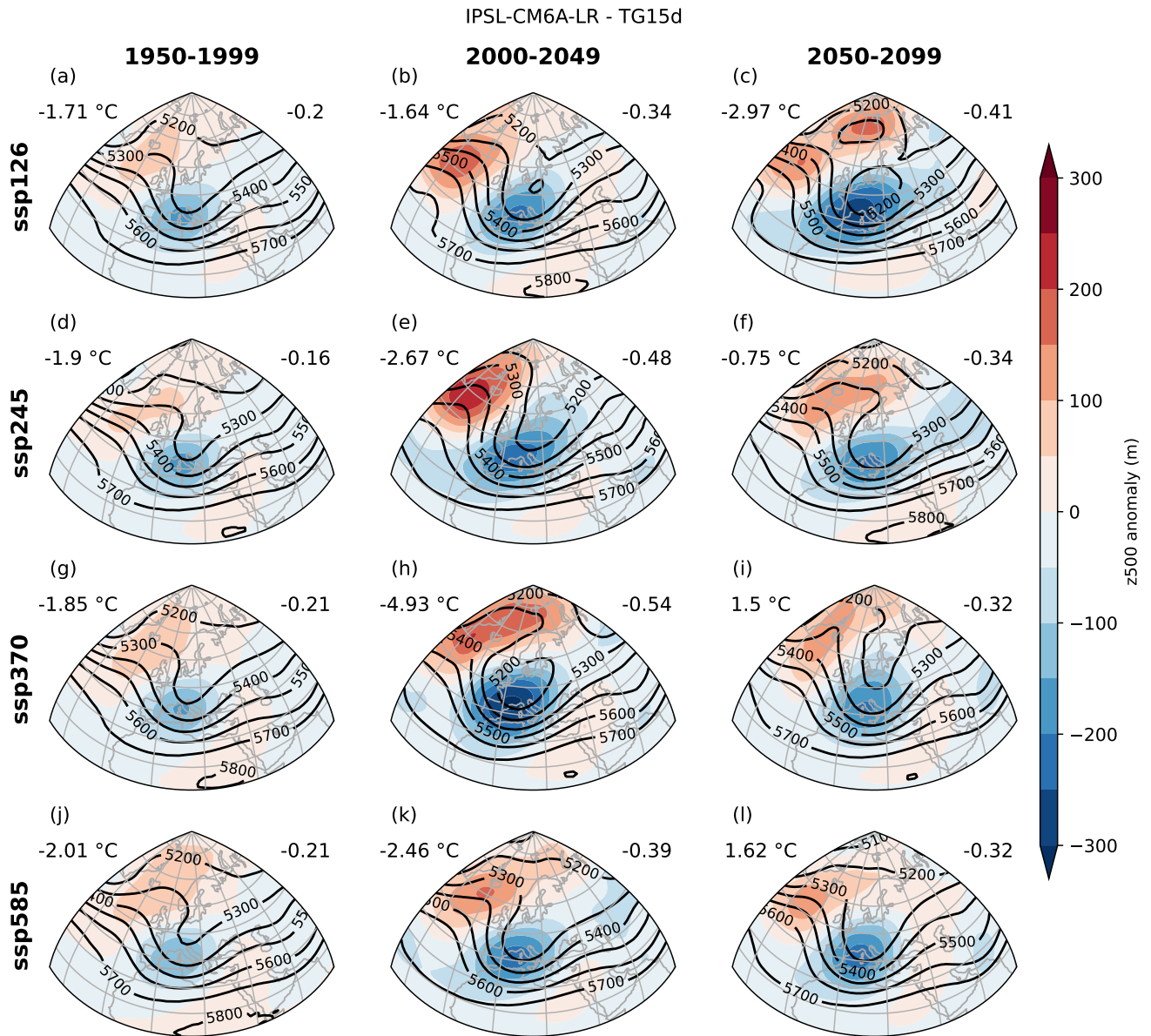
3   Z500 standard deviations maps

Fig. S2. Absolute values (contours, in m) and anomalies (shaded areas, in m) with respect to 1950-1999 of 500-hPa geopotential height (Z500) for the 10% coldest SWG simulations (i.e. 100 trajectories) for each period (columns) and SSP (rows) in FGOALS-g3.

4 SWG simulations with importance sampling on WCC index

Fig. S3. Absolute values (contours, in m) and anomalies (shaded areas, in m) with respect to 1950-1999 of 500-hPa geopotential height (Z500) for the 10% coldest SWG simulations (i.e. 100 trajectories) for each period (columns) and SSP (rows) in IPSL-CM6A-LR.

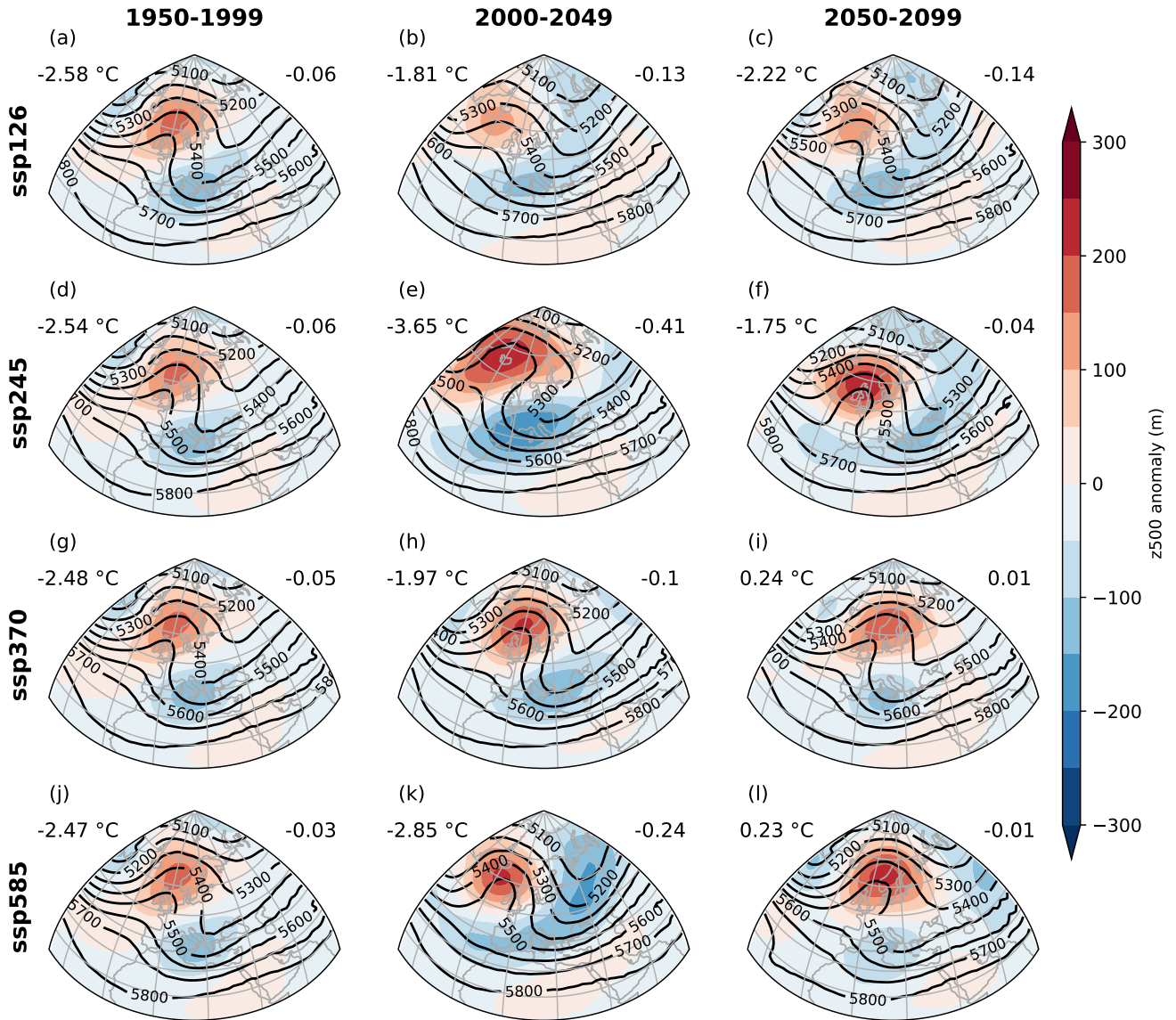*Code and data availability.* The ERA5 reanalysis data are publicly available at https://cds.climate.copernicus.eu/.

Fig. S4. Absolute values (contours, in m) and anomalies (shaded areas, in m) with respect to 1950-1999 of 500-hPa geopotential height (Z500) for the 10% coldest SWG simulations (i.e. 100 trajectories) for each period (columns) and SSP (rows) in MPI-ESM1-2-LR.
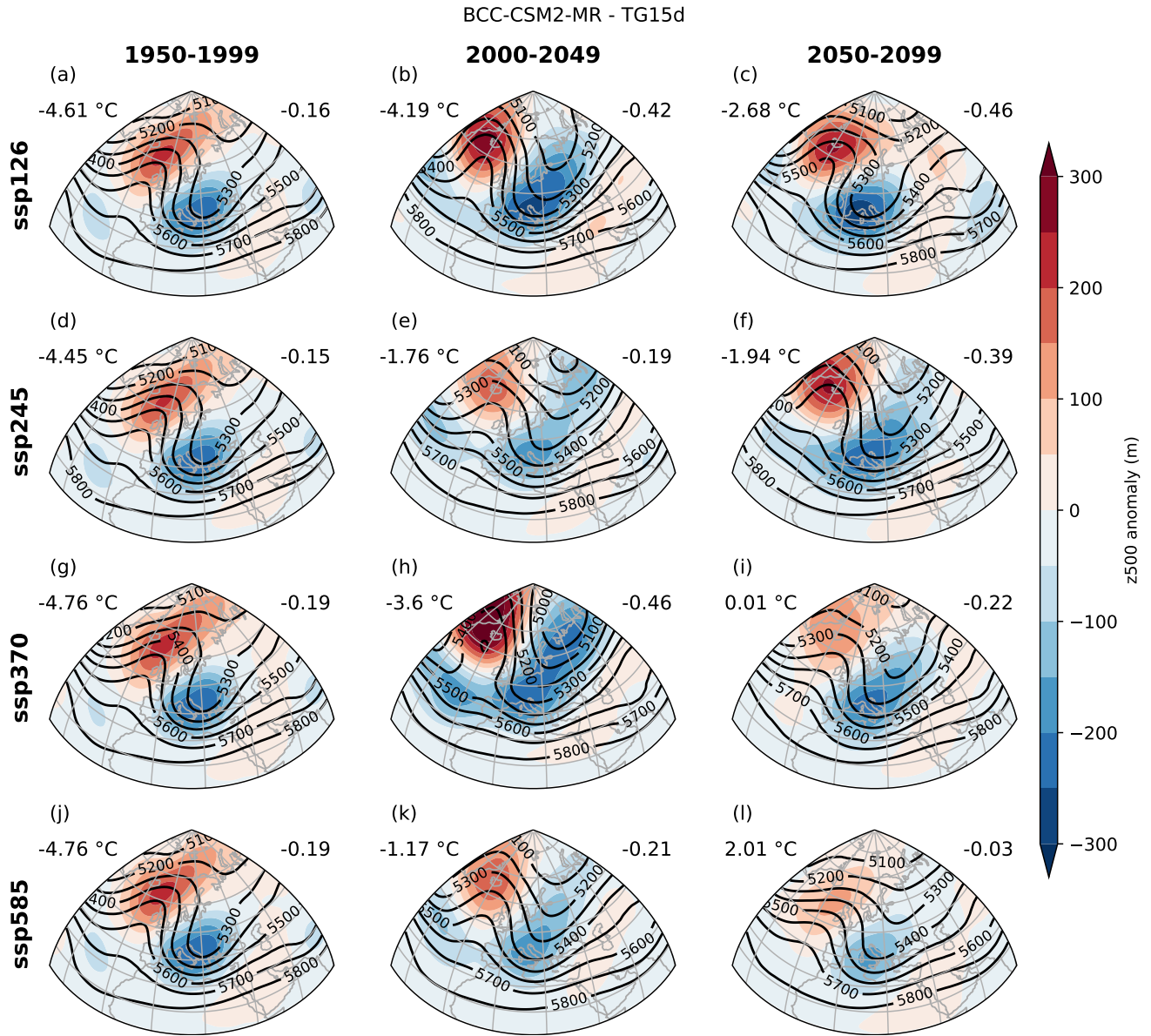
10 **References**

Fig. S5. Absolute values (contours, in m) and anomalies (shaded areas, in m) with respect to 1950-1999 of 500-hPa geopotential height (Z500) for the 10% coldest SWG simulations (i.e. 100 trajectories) for each period (columns) and SSP (rows) in BCC-CSM2-MR.
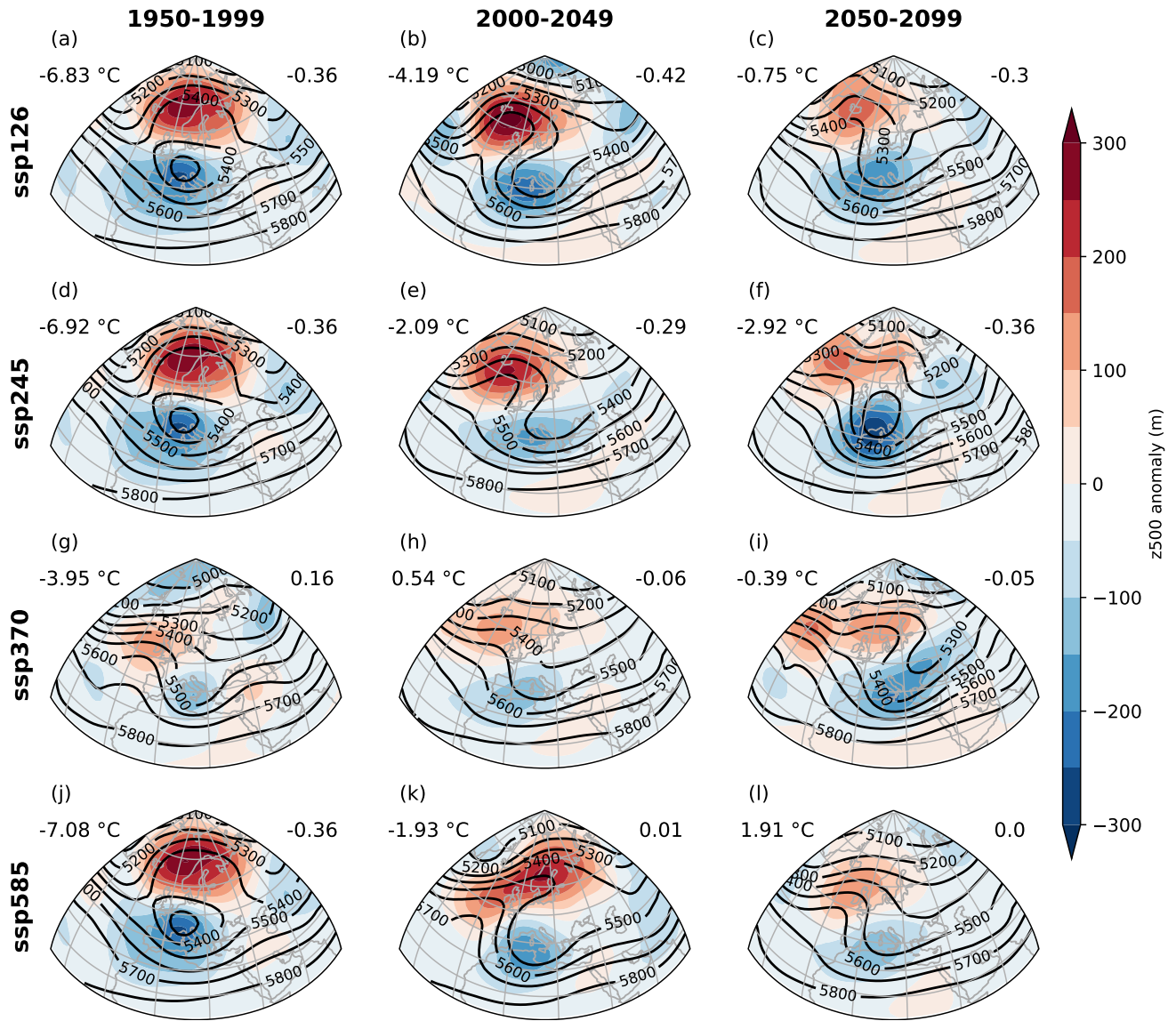
EC-Earth3 - TG15d

Fig. S6. Absolute values (contours, in m) and anomalies (shaded areas, in m) with respect to 1950-1999 of 500-hPa geopotential height (Z500) for the 10% coldest SWG simulations (i.e. 100 trajectories) for each period (columns) and SSP (rows) in EC-Earth3.
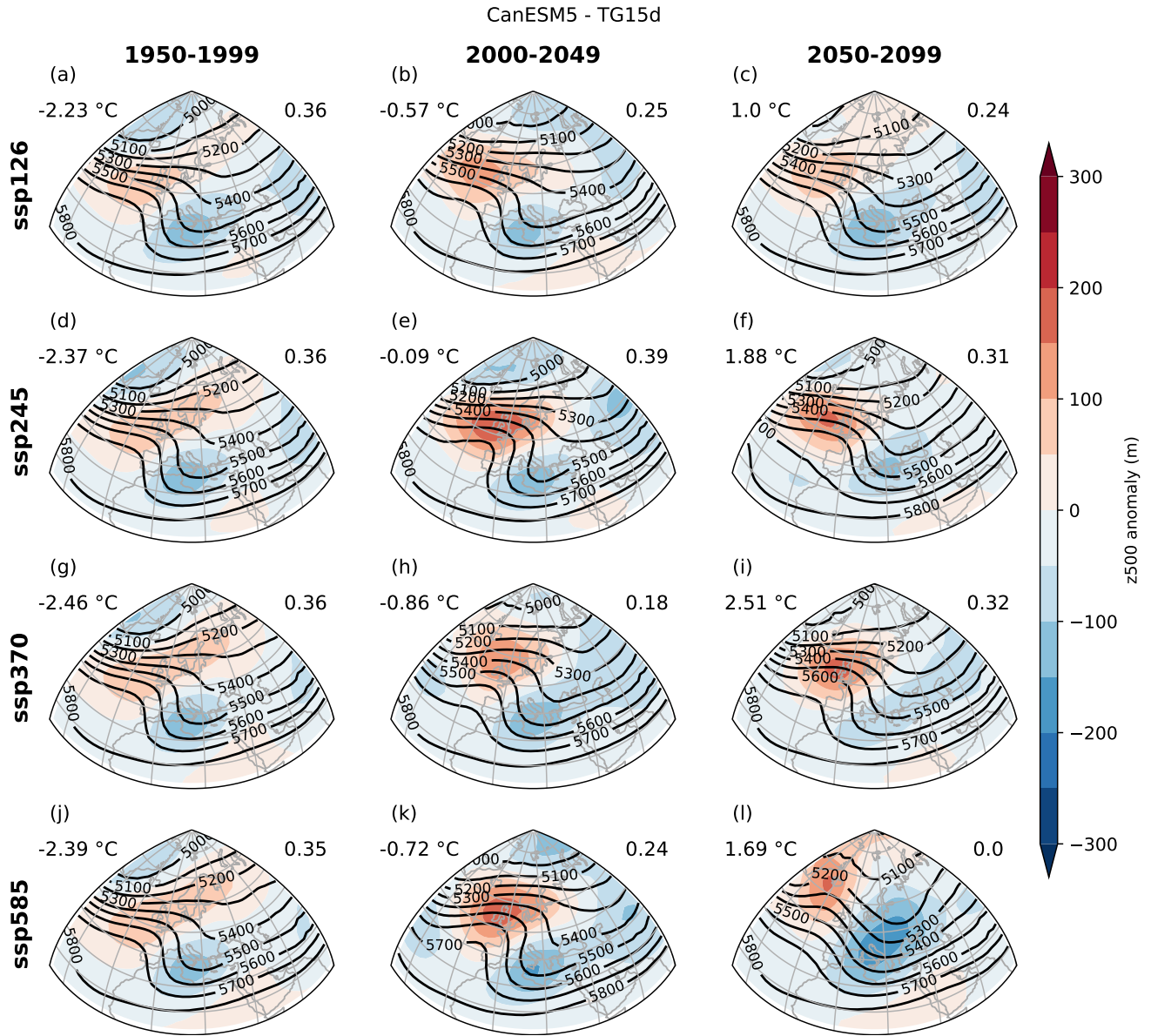
Fig. S7. Absolute values (contours, in m) and anomalies (shaded areas, in m) with respect to 1950-1999 of 500-hPa geopotential height (Z500) for the 10% coldest SWG simulations (i.e. 100 trajectories) for each period (columns) and SSP (rows) in CanESM5.
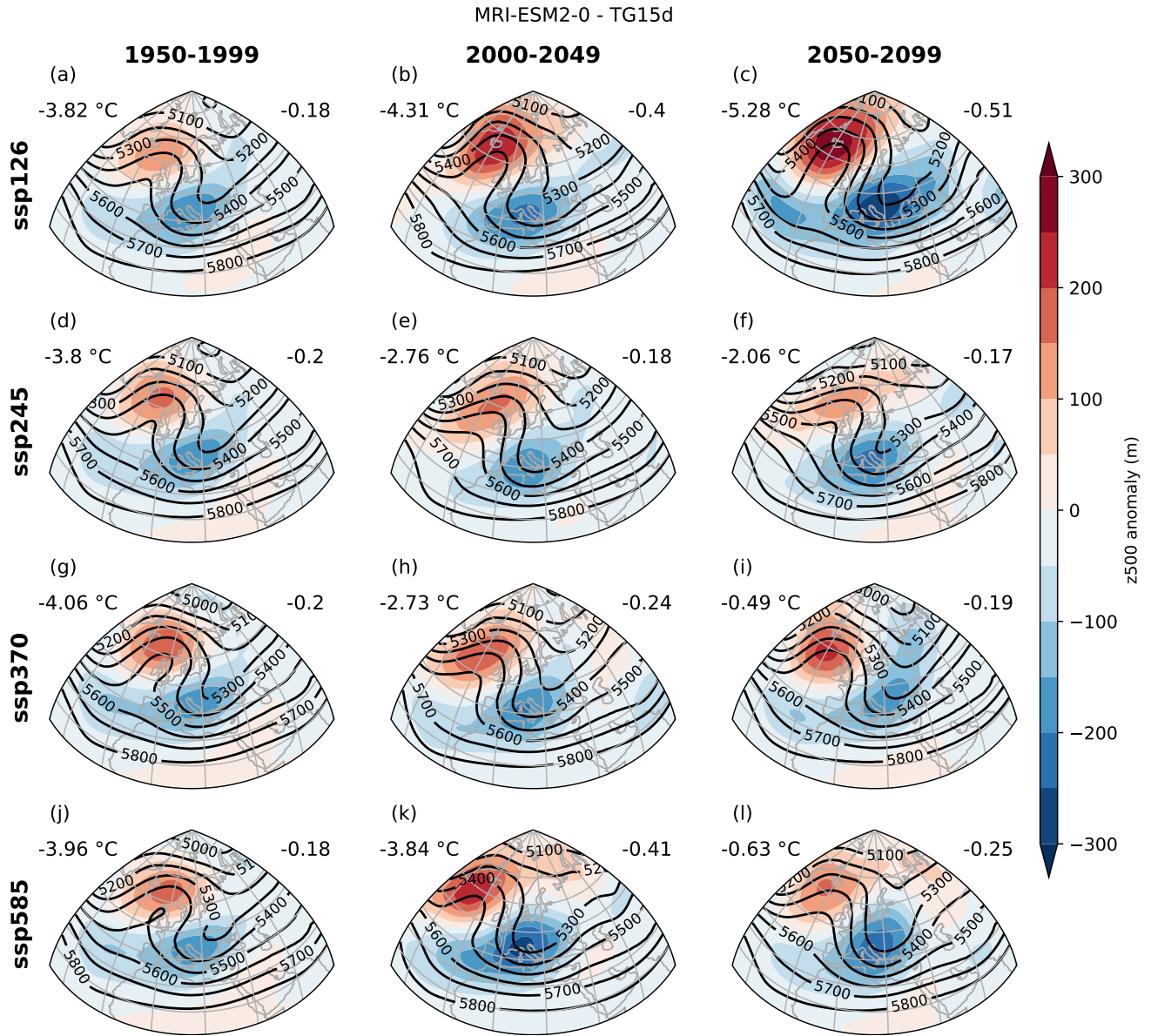
Fig. S8. Absolute values (contours, in m) and anomalies (shaded areas, in m) with respect to 1950-1999 of 500-hPa geopotential height (Z500) for the 10% coldest SWG simulations (i.e. 100 trajectories) for each period (columns) and SSP (rows) in MRI-ESM2-0.
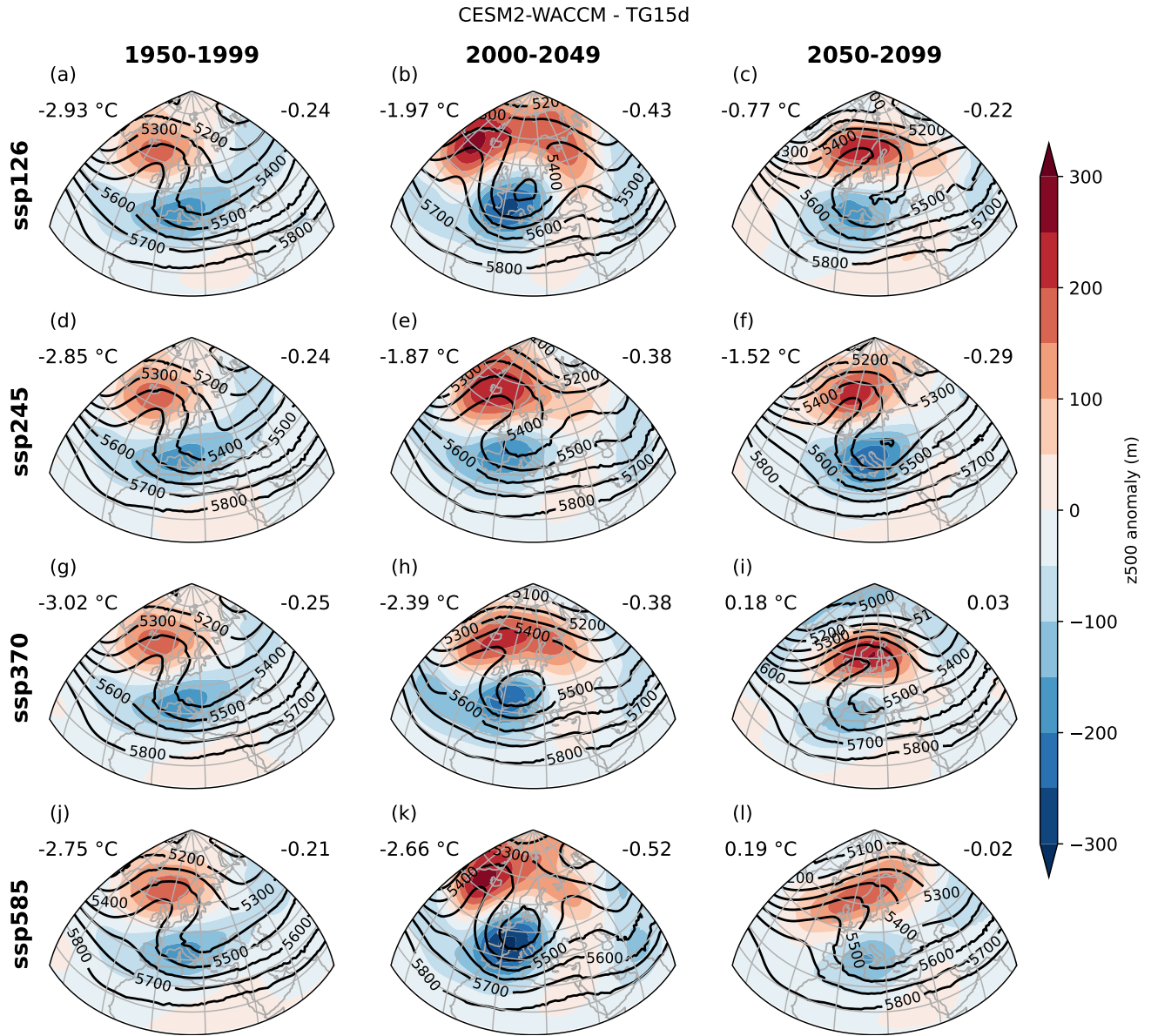
Fig. S9. Absolute values (contours, in m) and anomalies (shaded areas, in m) with respect to 1950-1999 of 500-hPa geopotential height (Z500) for the 10% coldest SWG simulations (i.e. 100 trajectories) for each period (columns) and SSP (rows) in CESM2-WACCM.
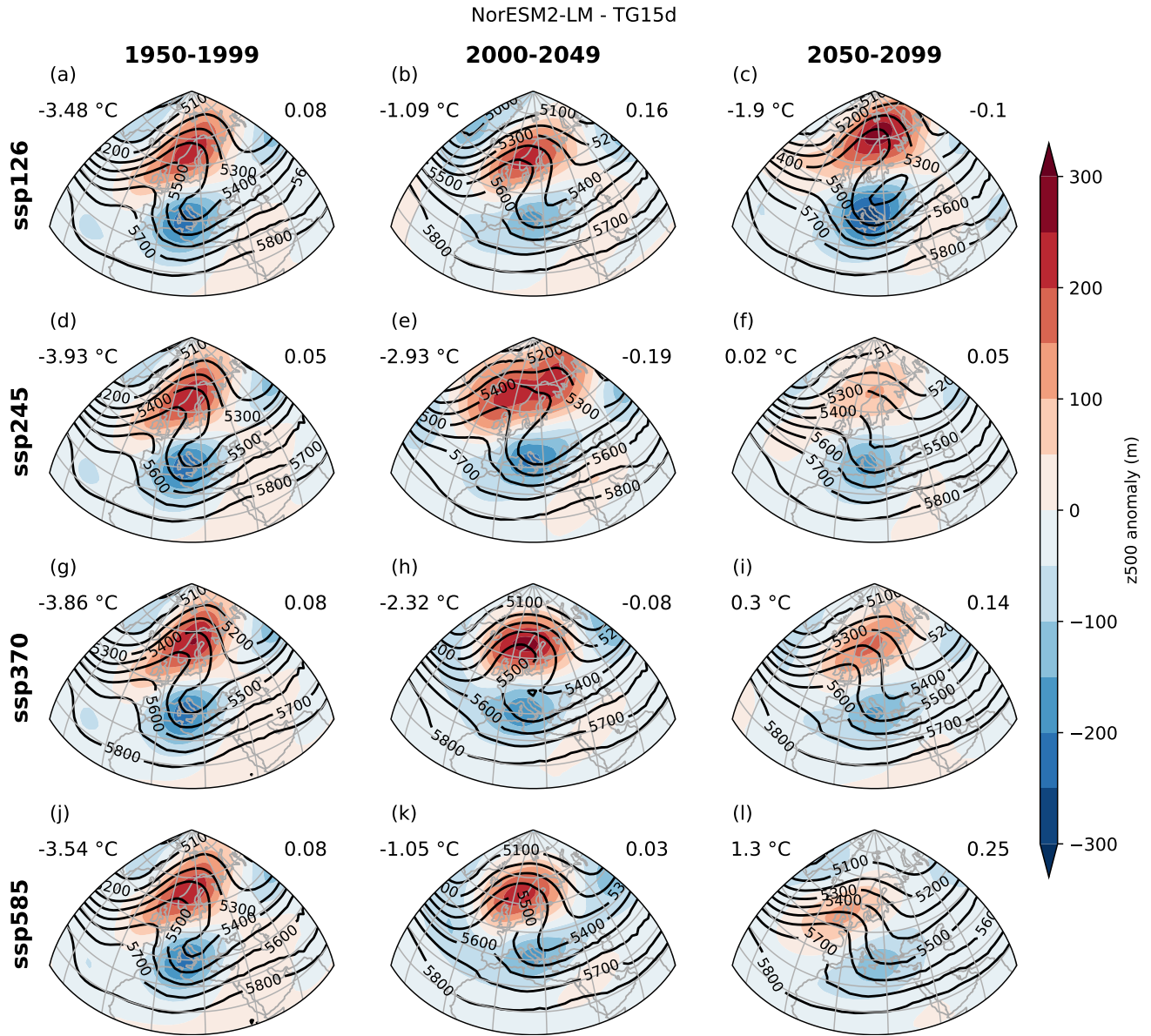
Fig. S10. Absolute values (contours, in m) and anomalies (shaded areas, in m) with respect to 1950-1999 of 500-hPa geopotential height (Z500) for the 10% coldest SWG simulations (i.e. 100 trajectories) for each period (columns) and SSP (rows) in NorESM2-LM.
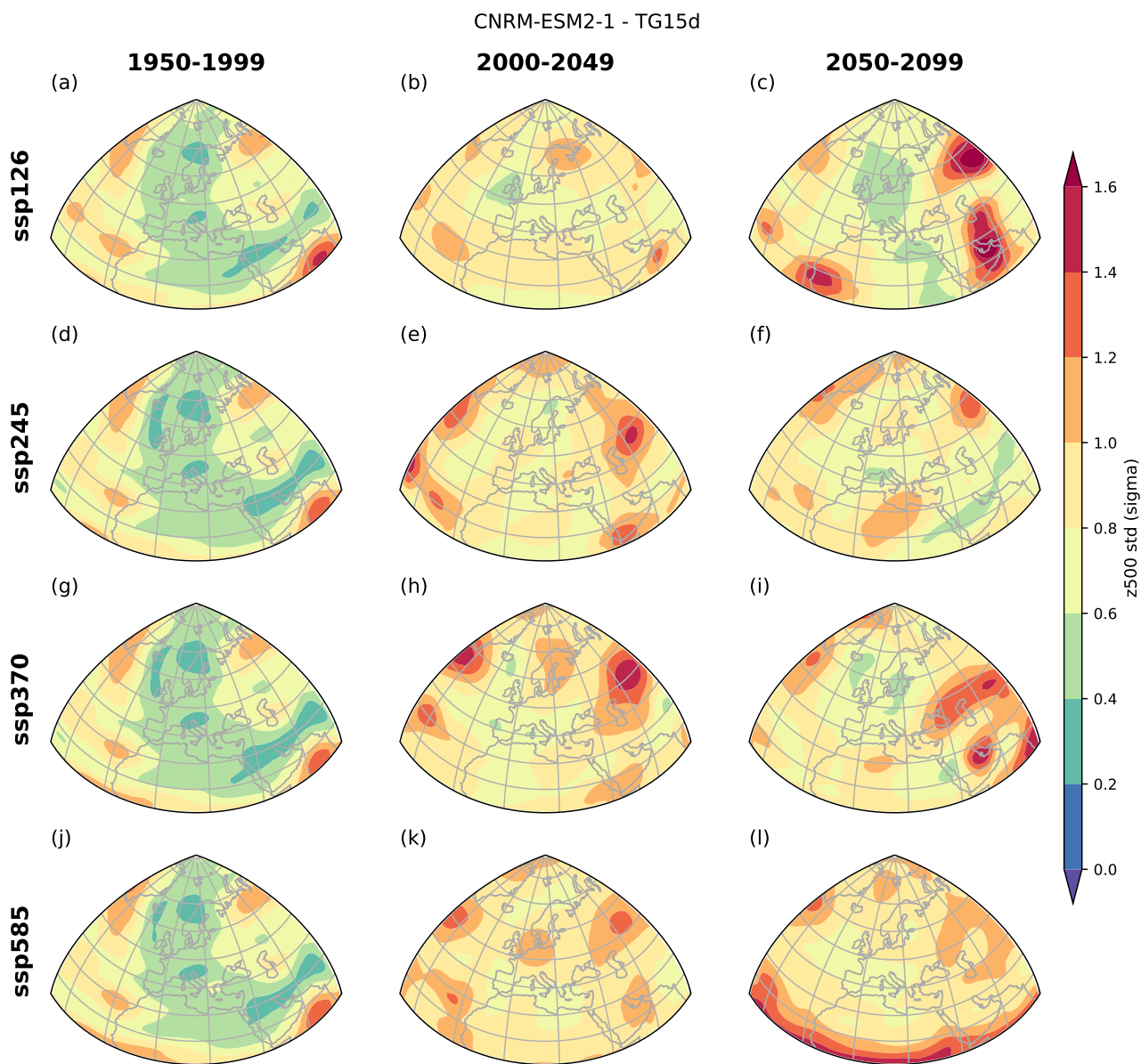
Fig. S11. Standardized standard deviation (shaded areas, σ) and anomalies with respect to 1950-1999 standard deviation of 500-hPa geopotential height (Z500) for the 10% coldest SWG simulations (i.e. 100 trajectories) for each period (columns) and SSP (rows) in CNRM-ESM2-1.
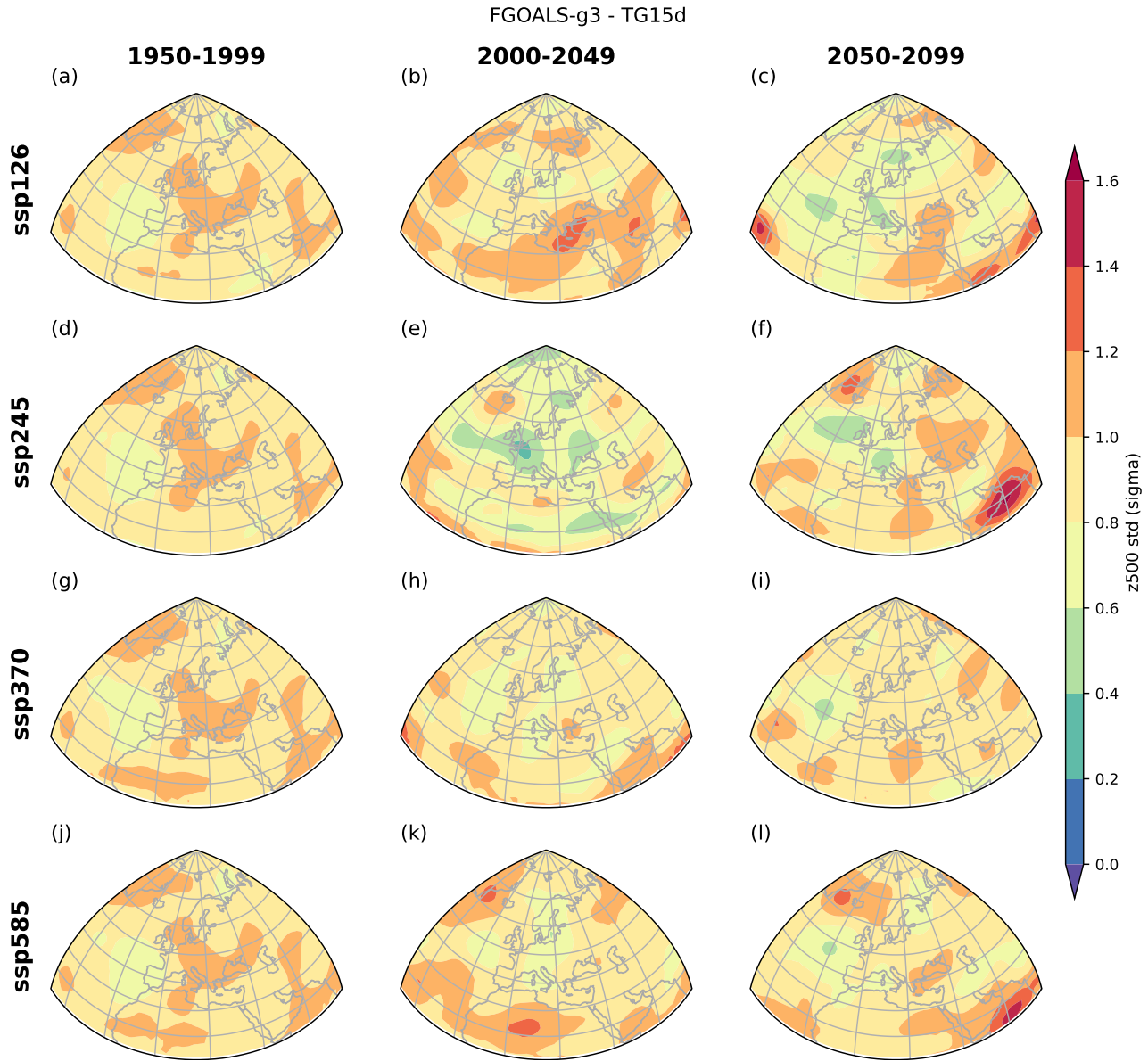
Fig. S12. Standardized standard deviation (shaded areas, σ) and anomalies with respect to 1950-1999 standard deviation of 500-hPa geopotential height (Z500) for the 10% coldest SWG simulations (i.e. 100 trajectories) for each period (columns) and SSP (rows) in FGOALS-g3.
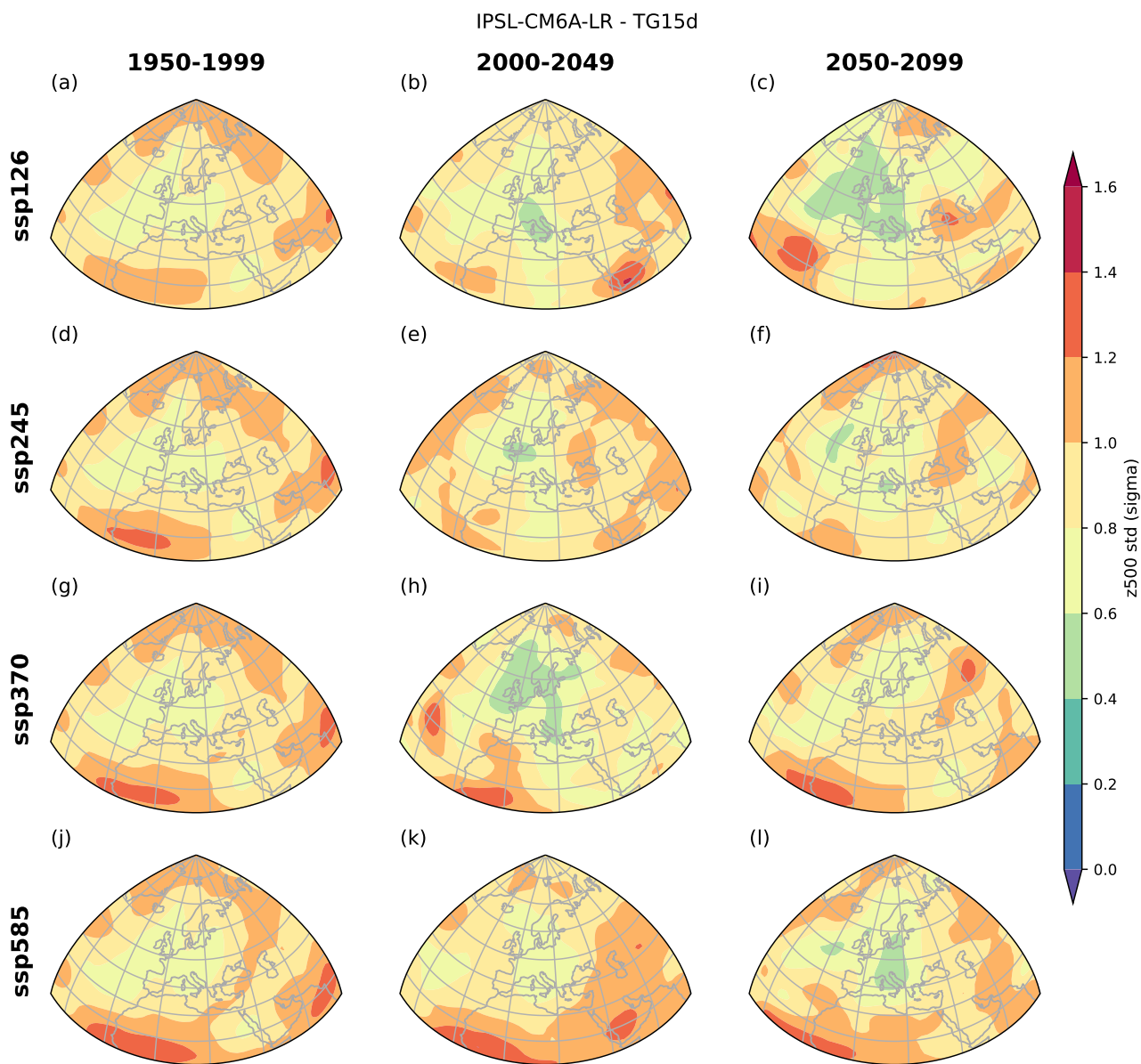
Fig. S13. Standardized standard deviation (shaded areas, σ) and anomalies with respect to 1950-1999 standard deviation of 500-hPa geopotential height (Z500) for the 10% coldest SWG simulations (i.e. 100 trajectories) for each period (columns) and SSP (rows) in IPSL-CM6A-LR.
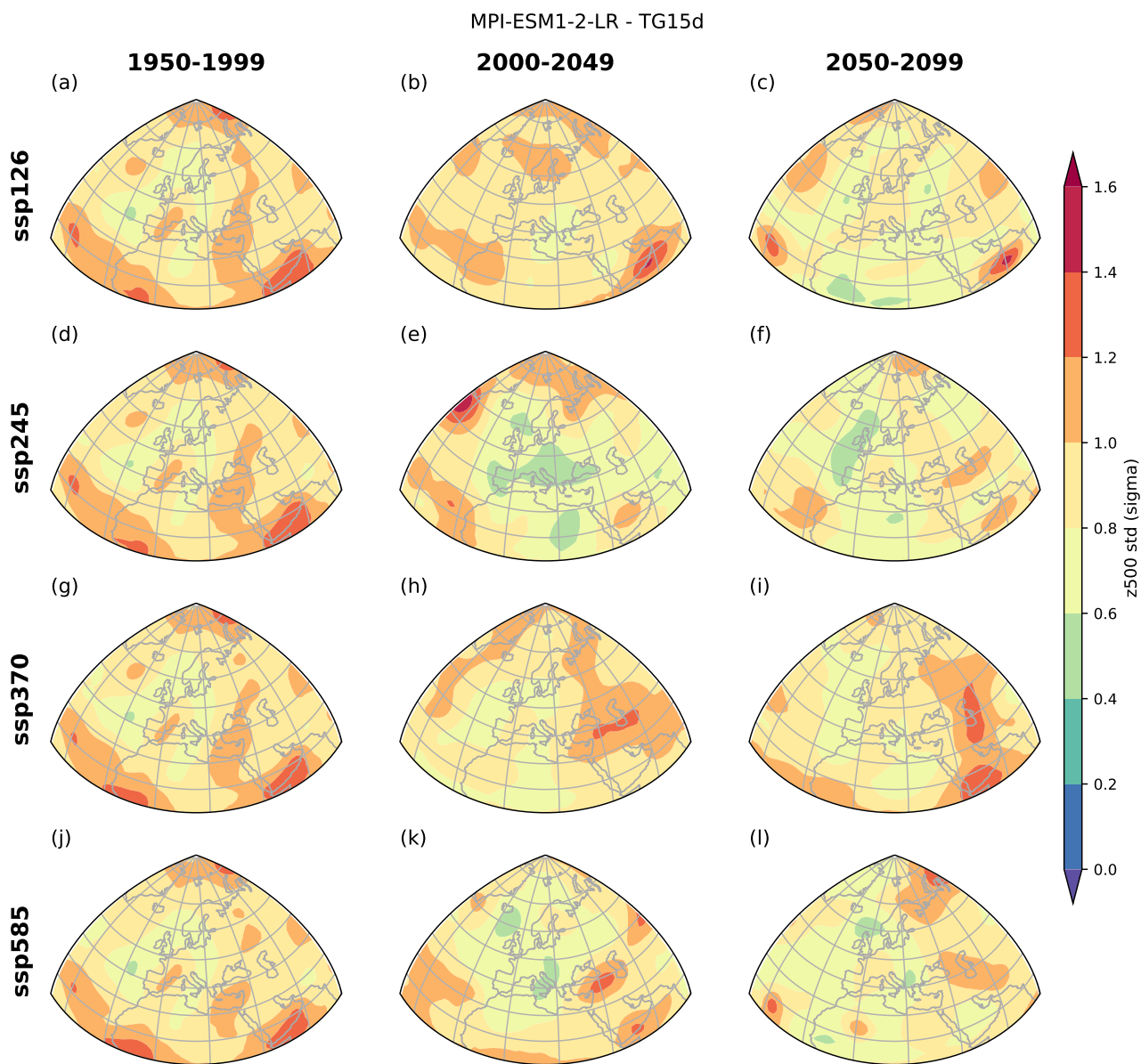
MPI-ESM1-2-LR - TG15d

Fig. S14. Standardized standard deviation (shaded areas, σ) and anomalies with respect to 1950-1999 standard deviation of 500-hPa geopotential height (Z500) for the 10% coldest SWG simulations (i.e. 100 trajectories) for each period (columns) and SSP (rows) in MPI-ESM1-2-LR.
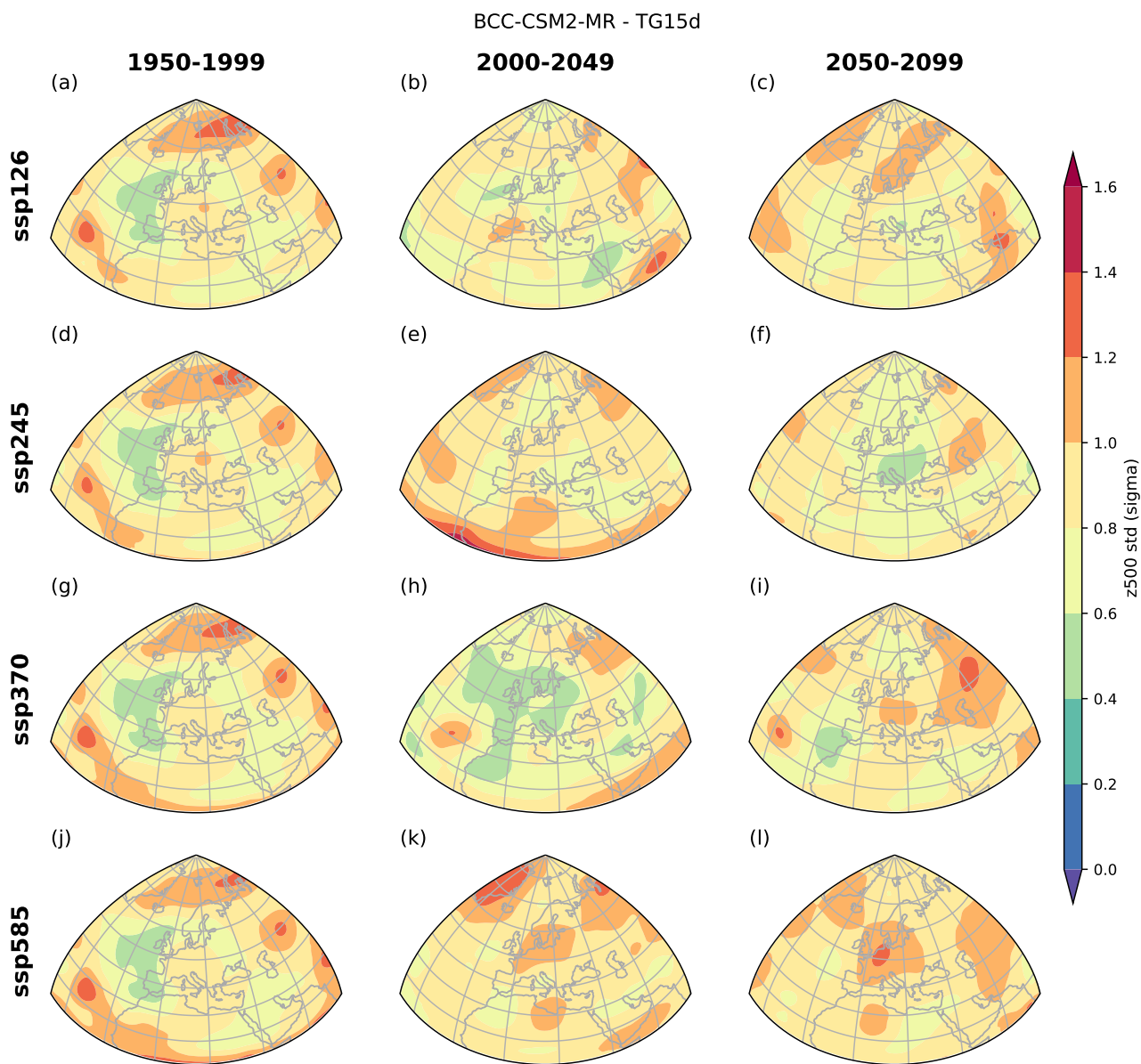
BCC-CSM2-MR - TG15d

Fig. S15. Standardized standard deviation (shaded areas, σ) and anomalies with respect to 1950-1999 standard deviation of 500-hPa geopotential height (Z500) for the 10% coldest SWG simulations (i.e. 100 trajectories) for each period (columns) and SSP (rows) in BCC-CSM2-MR.
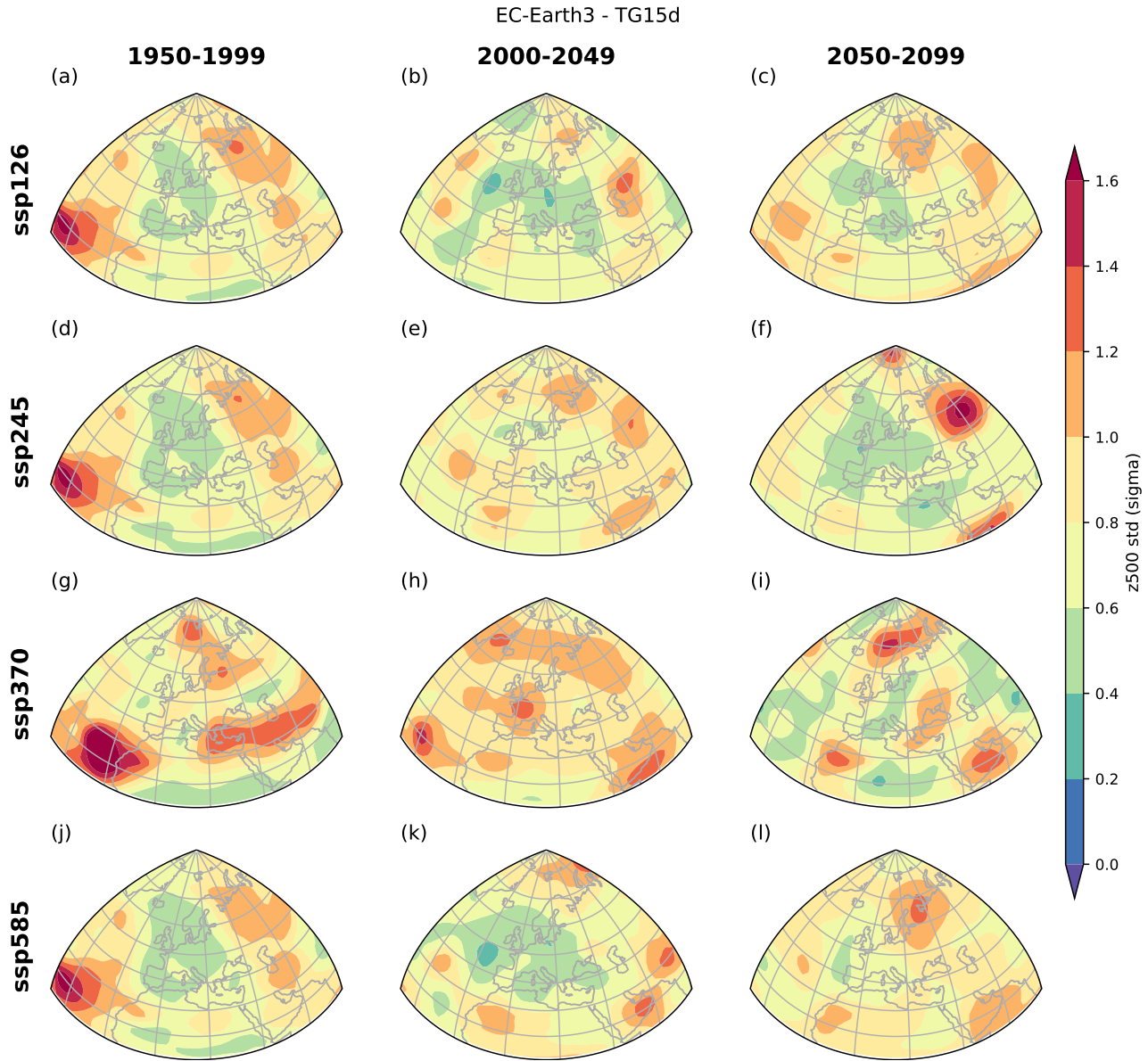
Fig. S16. Standardized standard deviation (shaded areas, σ) and anomalies with respect to 1950-1999 standard deviation of 500-hPa geopotential height (Z500) for the 10% coldest SWG simulations (i.e. 100 trajectories) for each period (columns) and SSP (rows) in EC-Earth3.
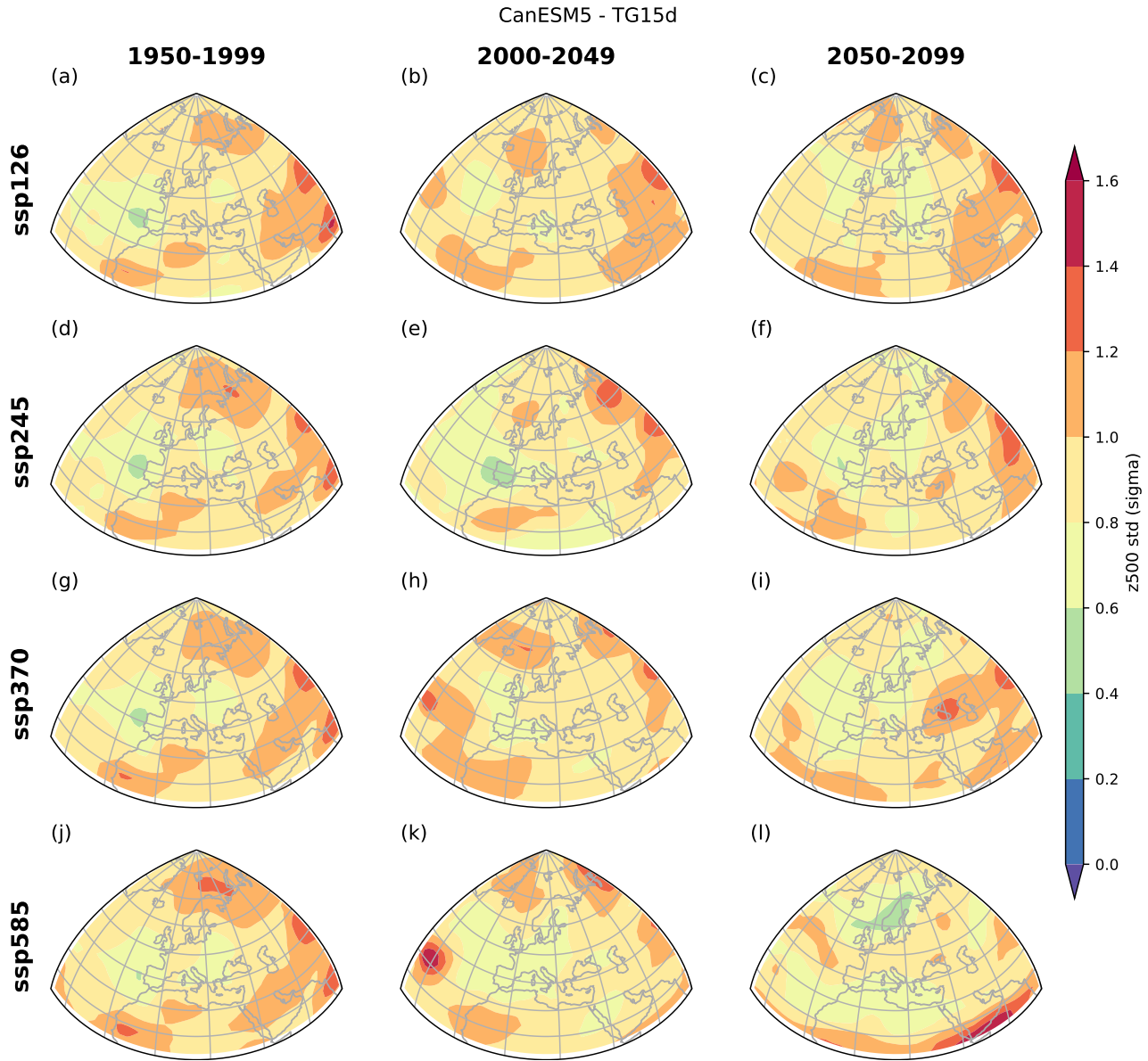
Fig. S17. Standardized standard deviation (shaded areas, σ) and anomalies with respect to 1950-1999 standard deviation of 500-hPa geopotential height (Z500) for the 10% coldest SWG simulations (i.e. 100 trajectories) for each period (columns) and SSP (rows) in CanESM5.
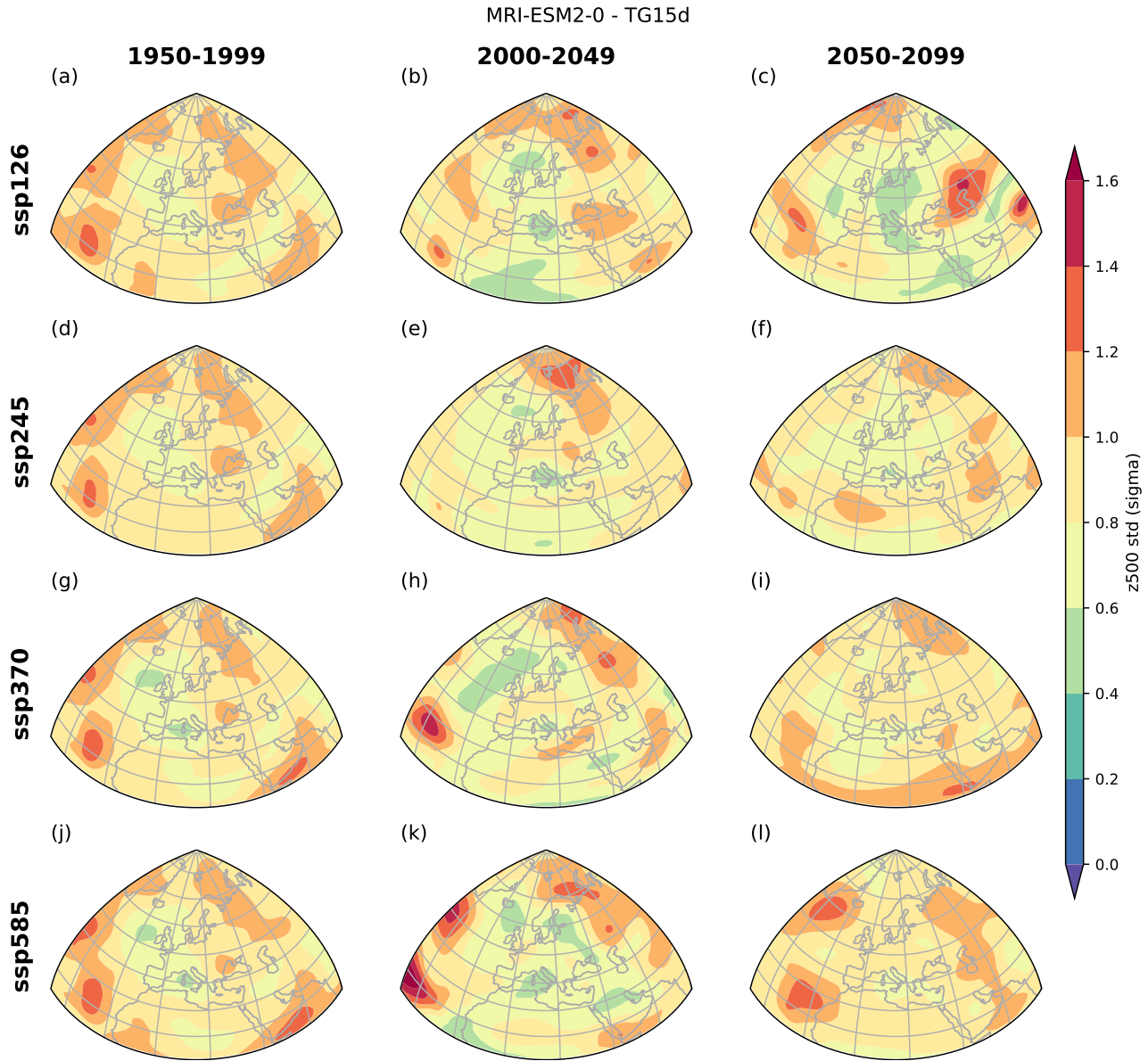
Fig. S18. Standardized standard deviation (shaded areas, σ) and anomalies with respect to 1950-1999 standard deviation of 500-hPa geopotential height (Z500) for the 10% coldest SWG simulations (i.e. 100 trajectories) for each period (columns) and SSP (rows) in MRI-ESM2-0.
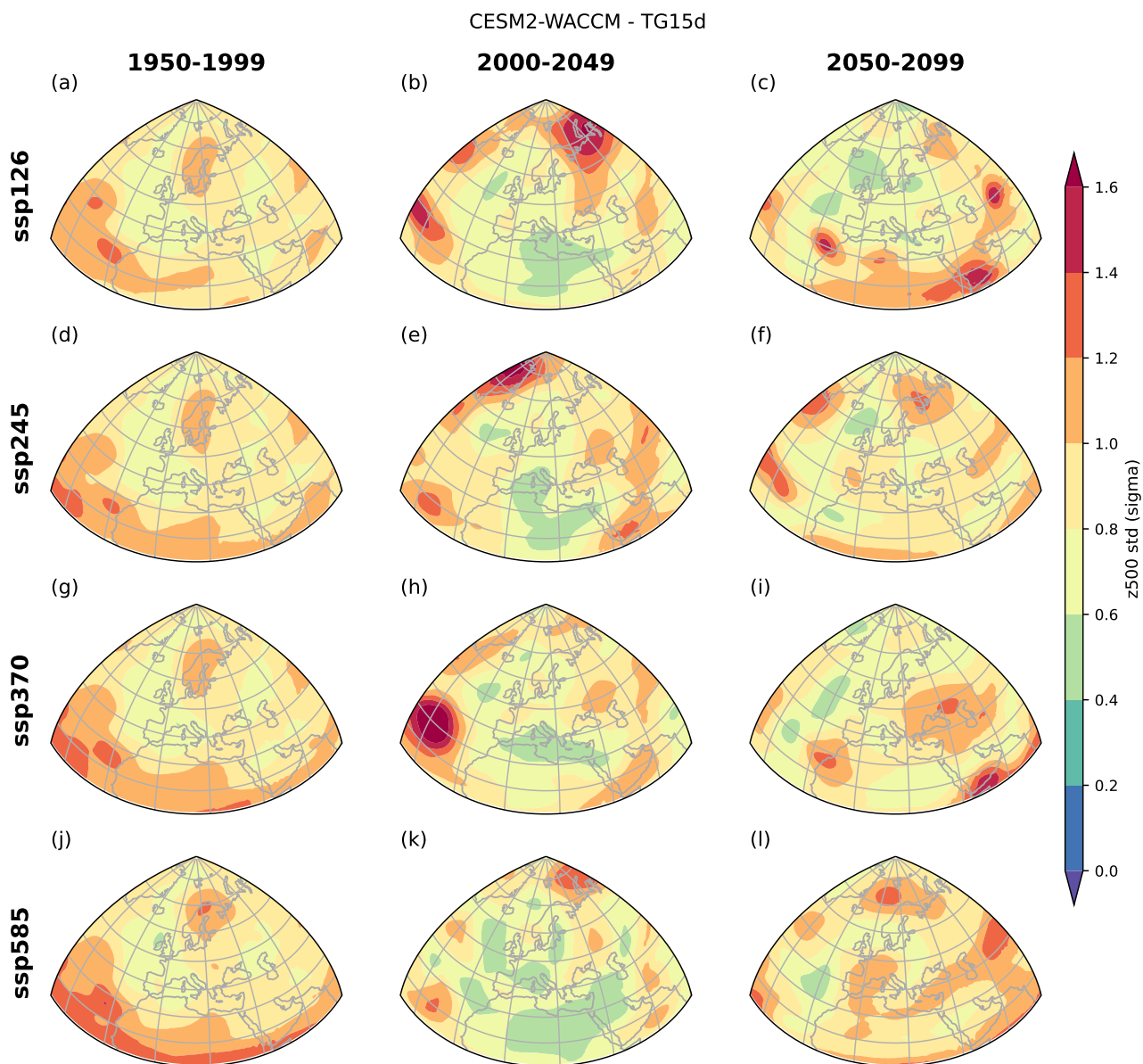
Fig. S19. Standardized standard deviation (shaded areas, σ) and anomalies with respect to 1950-1999 standard deviation of 500-hPa geopotential height (Z500) for the 10% coldest SWG simulations (i.e. 100 trajectories) for each period (columns) and SSP (rows) in CESM2-WACCM.
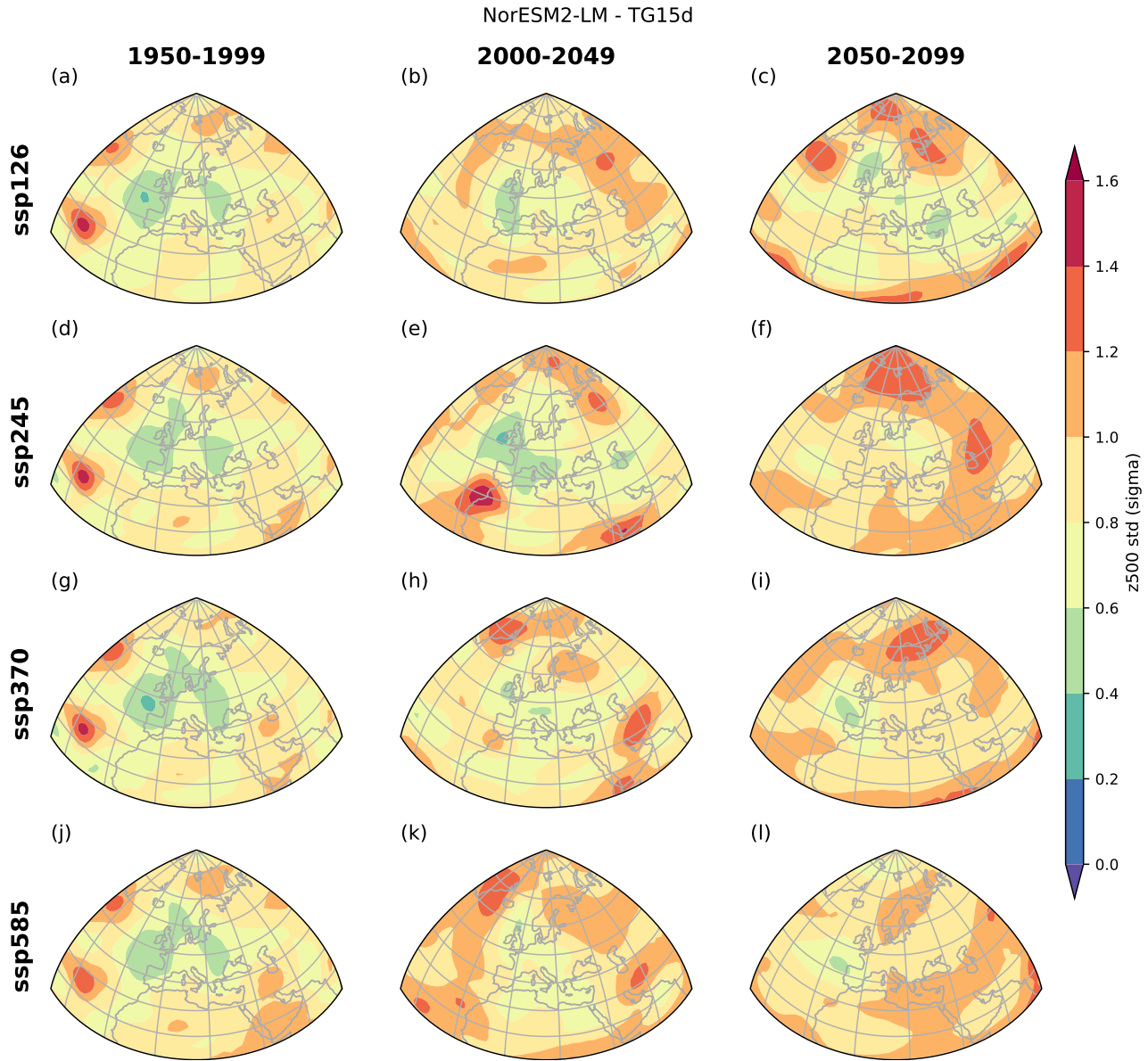
Fig. S20. Standardized standard deviation (shaded areas, σ) and anomalies with respect to 1950-1999 standard deviation of 500-hPa geopotential height (Z500) for the 10% coldest SWG simulations (i.e. 100 trajectories) for each period (columns) and SSP (rows) in NorESM2-LM.
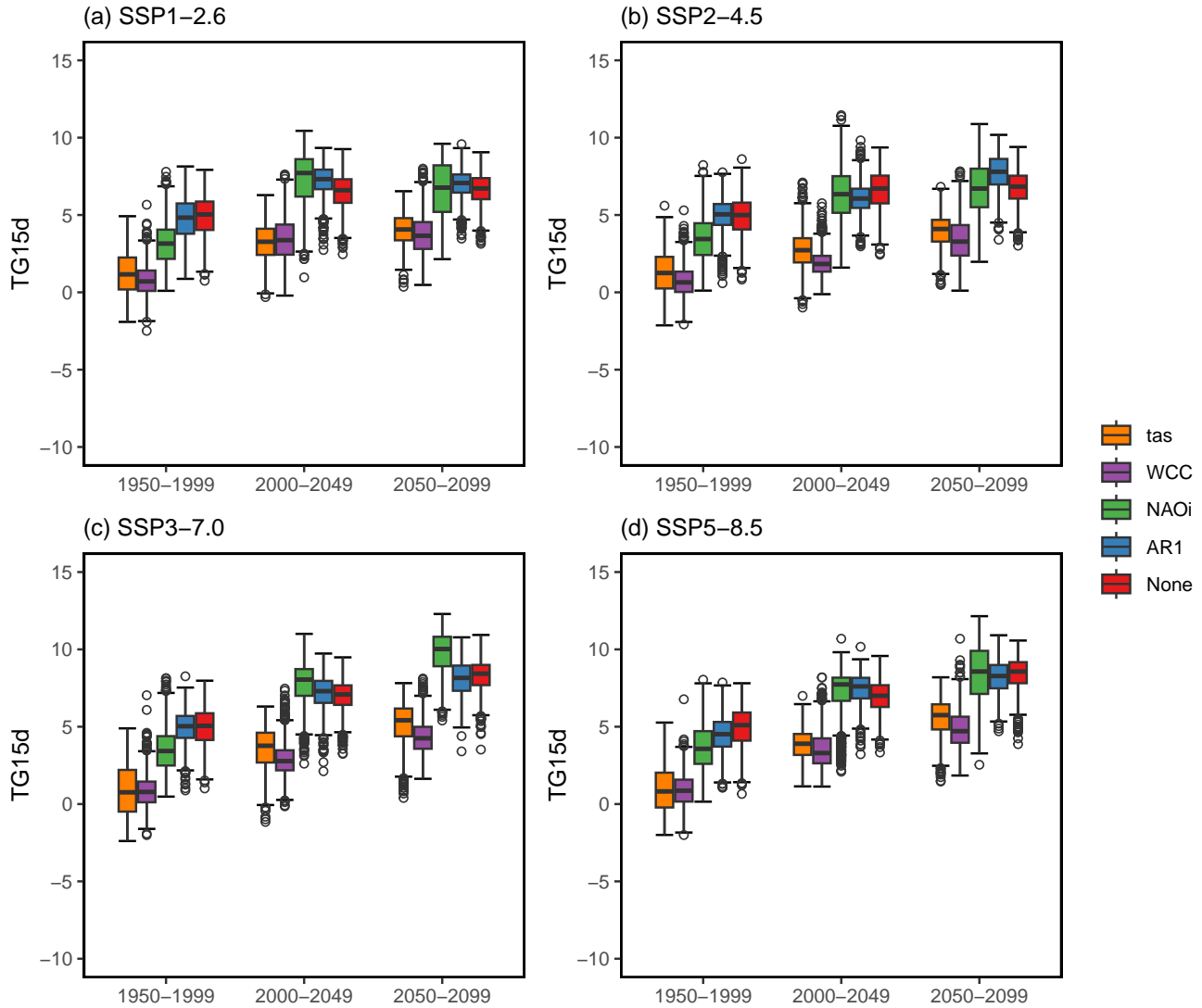
Fig. S21. Temperature (TG15d) distribution of 1000 SWG simulations for four SSPs (a-d) and three climate periods (left to right) depending on the variable used for importance sampling (colours) in CNRM-ESM2-1. Temperatures are adjusted by the median DJF temperature bias. In the box plots, the boxes represent the median ($q50$), with the lower and upper hinges denoting the first ($q25$) and third ($q75$) quartiles, respectively. The upper whiskers are defined as $\min[\max(T), q75 + 1.5 \times (q75 - q25)]$, while the lower whiskers are formulated symmetrically. The individual points in the plot correspond to the outlying values that exceed the upper whisker or fall below the lower whisker.
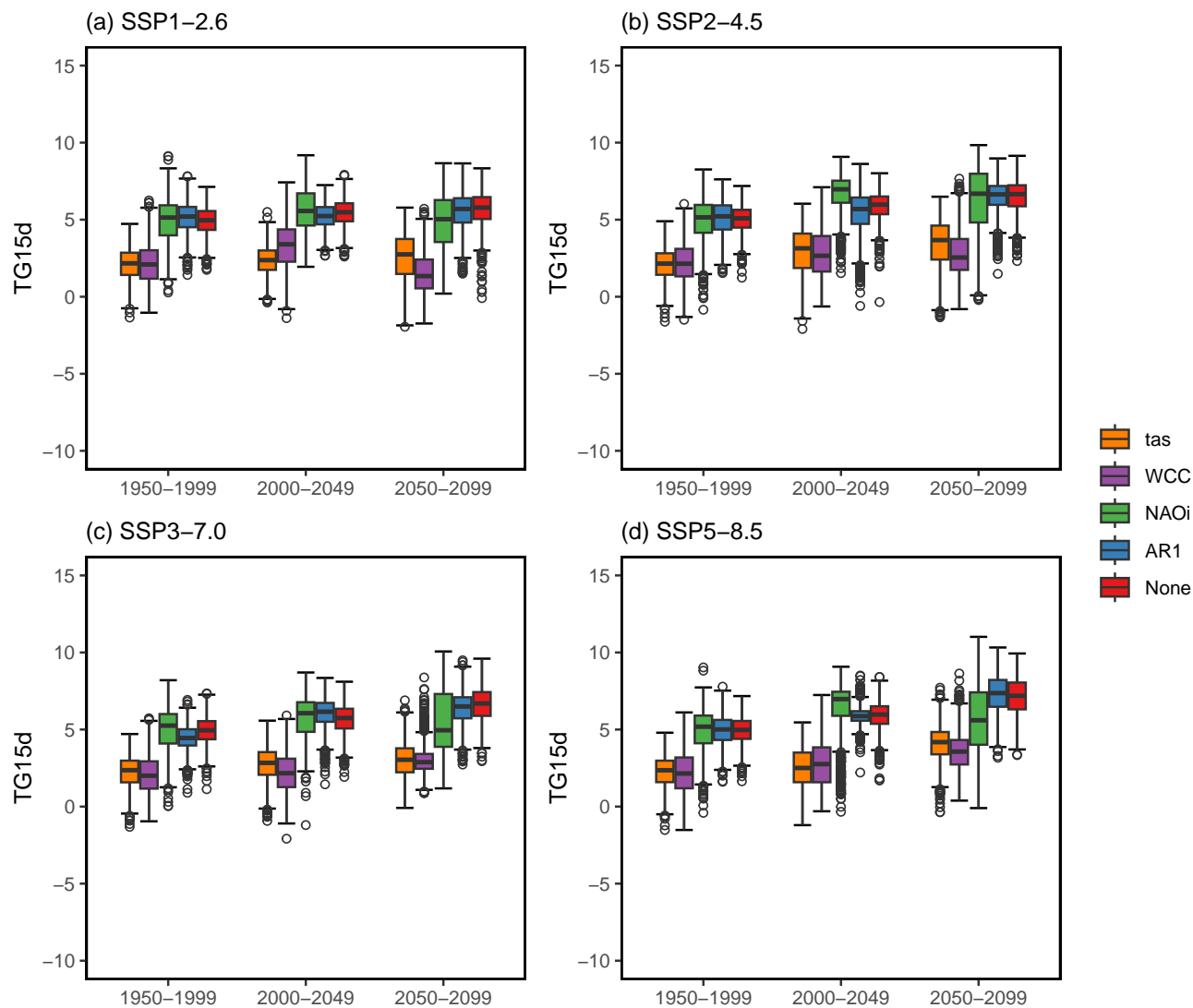
Fig. S22. Temperature (TG15d) distribution of 1000 SWG simulations for four SSPs (a-d) and three climate periods (left to right) depending on the variable used for importance sampling (colours) in FGOALS-g3. Temperatures are adjusted by the median DJF temperature bias. Boxplots are as defined in Fig. S21.
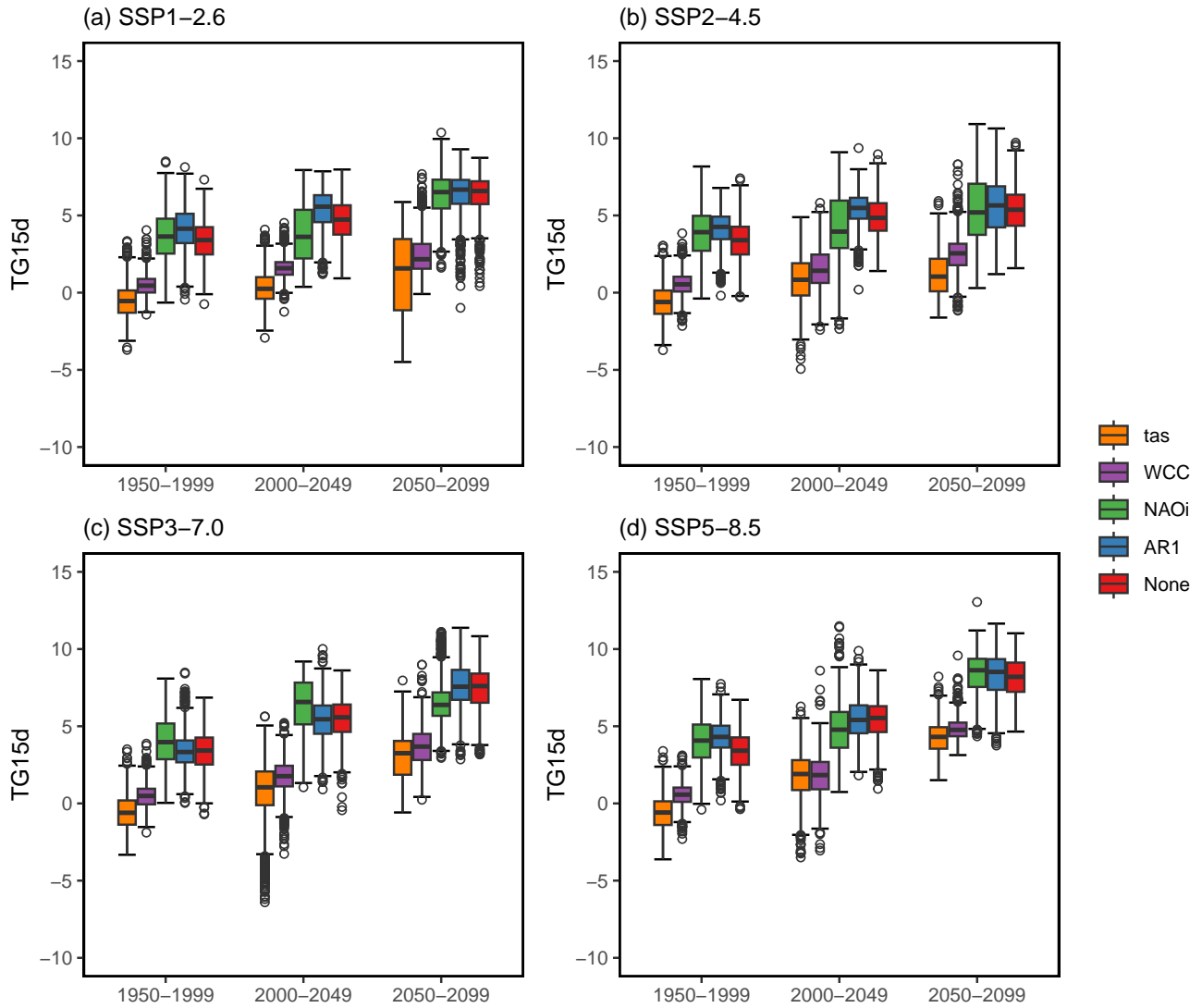
Fig. S23. Temperature (TG15d) distribution of 1000 SWG simulations for four SSPs (a-d) and three climate periods (left to right) depending on the variable used for importance sampling (colours) in IPSL-CM6A-LR. Temperatures are adjusted by the median DJF temperature bias. Boxplots are as defined in Fig. S21.
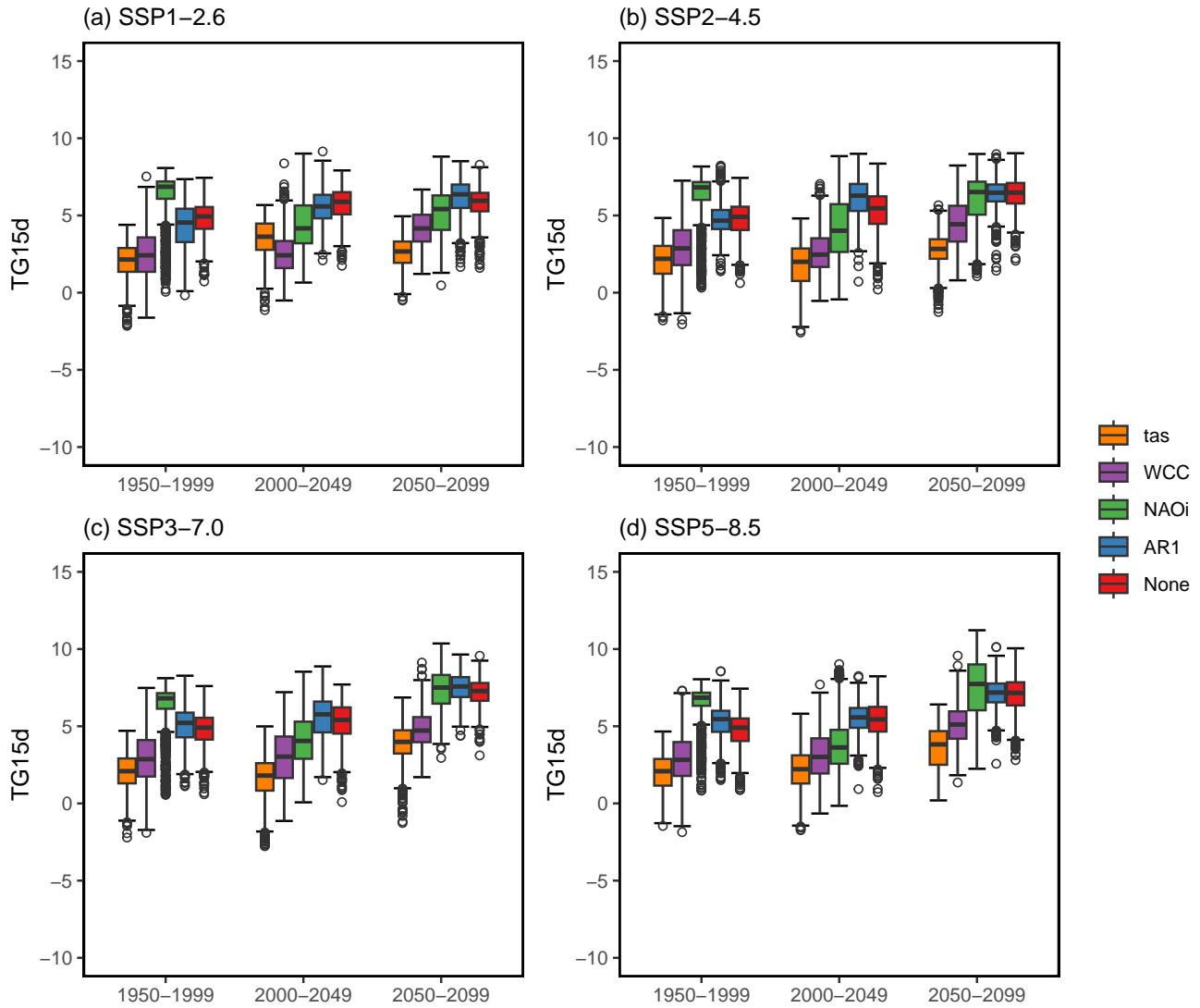
Fig. S24. Temperature (TG15d) distribution of 1000 SWG simulations for four SSPs (a-d) and three climate periods (left to right) depending on the variable used for importance sampling (colours) in MPI-ESM1-2-LR. Temperatures are adjusted by the median DJF temperature bias. Boxplots are as defined in Fig. S21.
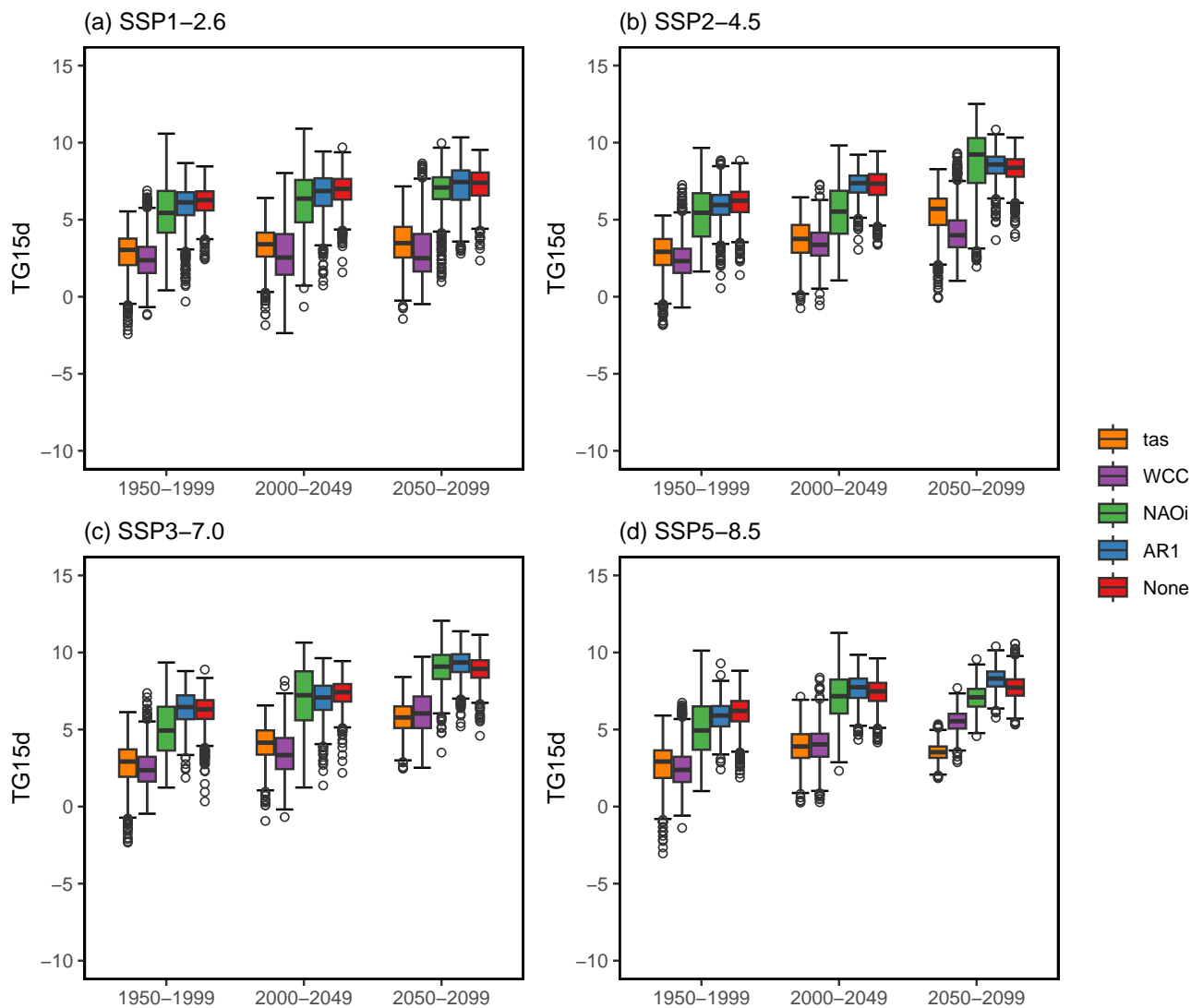
Fig. S25. Temperature (TG15d) distribution of 1000 SWG simulations for four SSPs (a-d) and three climate periods (left to right) depending on the variable used for importance sampling (colours) in BCC-CSM2-MR. Temperatures are adjusted by the median DJF temperature bias. Boxplots are as defined in Fig. S21.
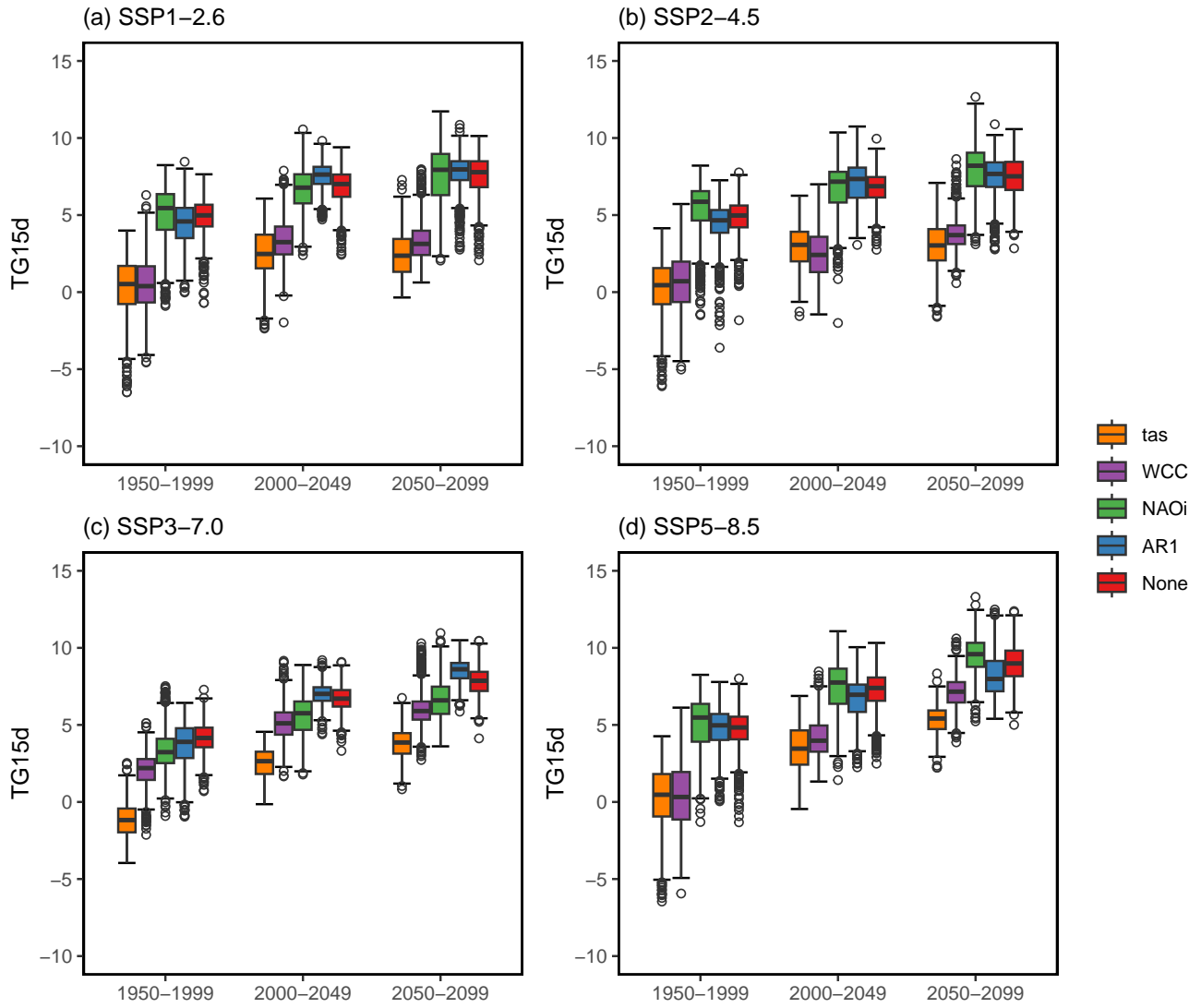
Fig. S26. Temperature (TG15d) distribution of 1000 SWG simulations for four SSPs (a-d) and three climate periods (left to right) depending on the variable used for importance sampling (colours) in EC-Earth3. Temperatures are adjusted by the median DJF temperature bias. Boxplots are as defined in Fig. S21.
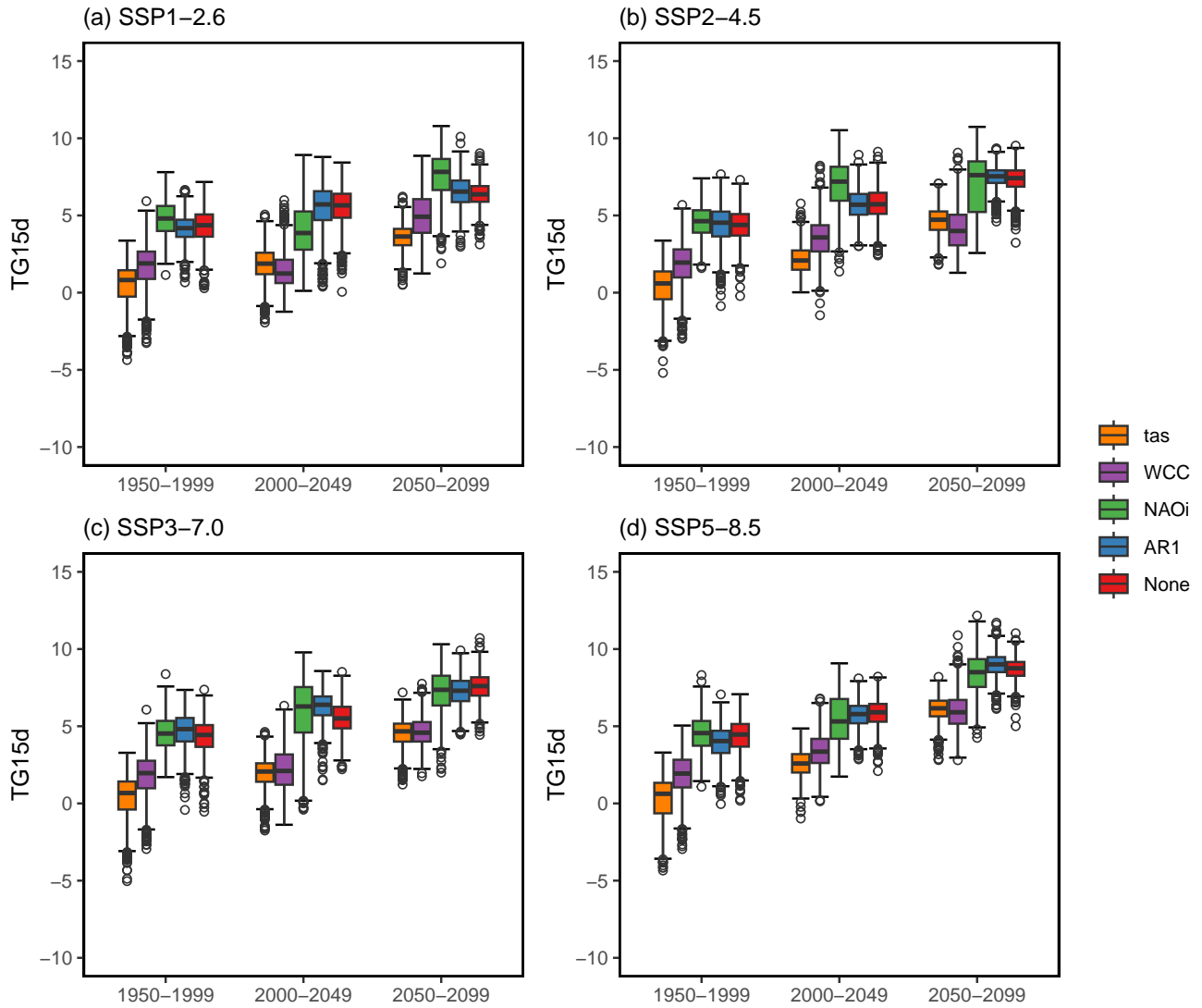
Fig. S27. Temperature (TG15d) distribution of 1000 SWG simulations for four SSPs (a-d) and three climate periods (left to right) depending on the variable used for importance sampling (colours) in CanESM5. Temperatures are adjusted by the median DJF temperature bias. Boxplots are as defined in Fig. S21.
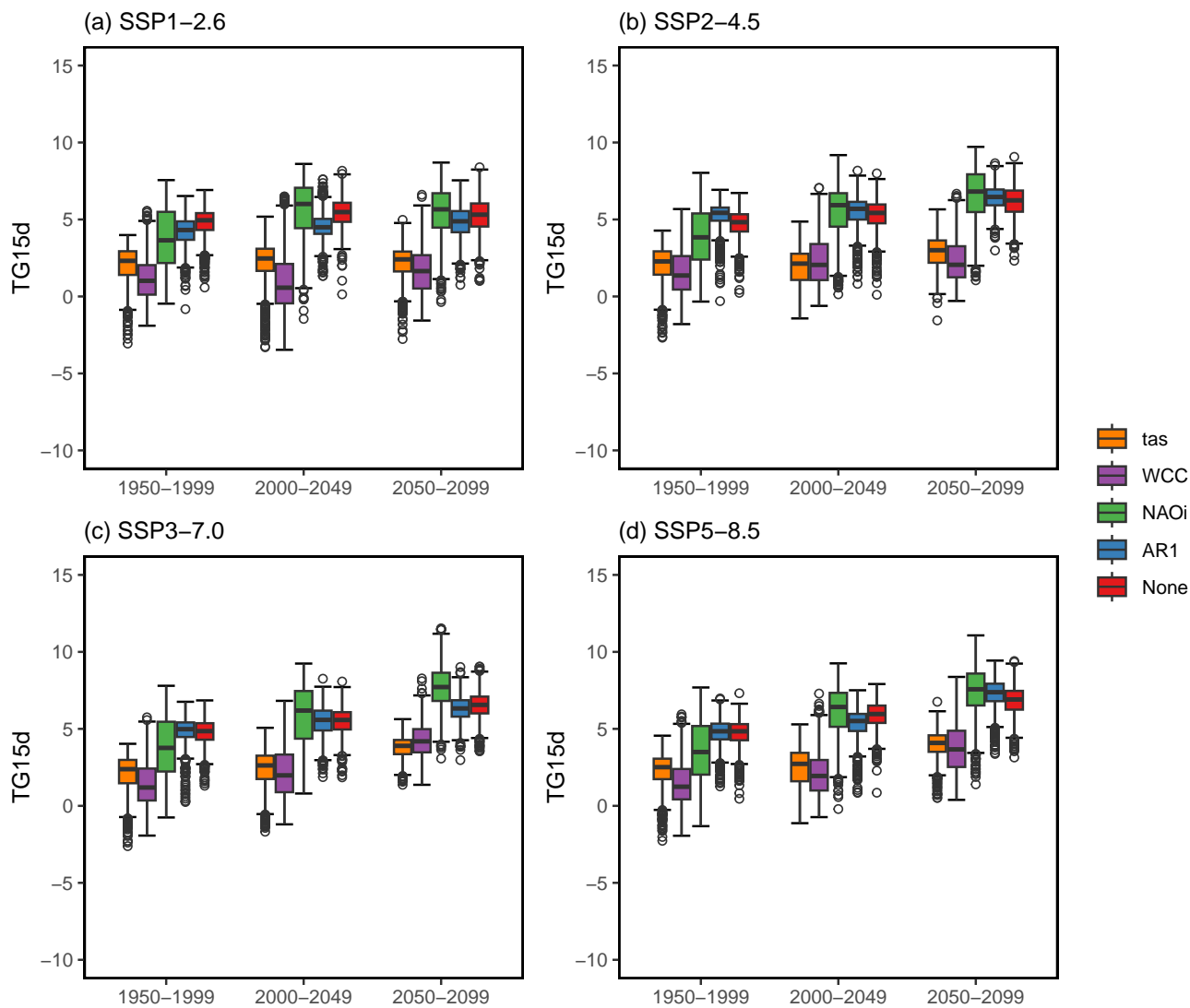
Fig. S28. Temperature (TG15d) distribution of 1000 SWG simulations for four SSPs (a-d) and three climate periods (left to right) depending on the variable used for importance sampling (colours) in MRI-ESM2-0. Temperatures are adjusted by the median DJF temperature bias. Boxplots are as defined in Fig. S21.
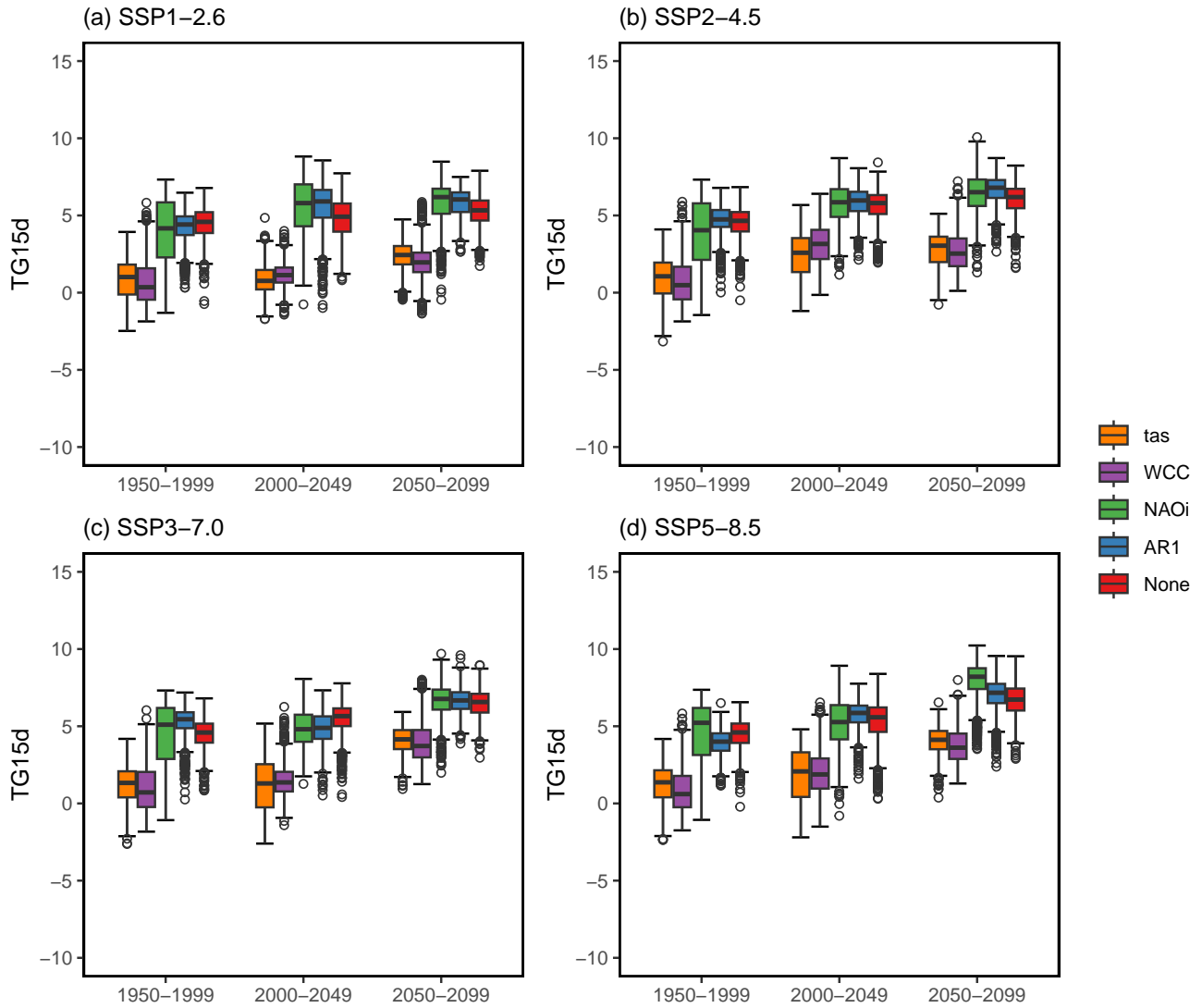
Fig. S29. Temperature (TG15d) distribution of 1000 SWG simulations for four SSPs (a-d) and three climate periods (left to right) depending on the variable used for importance sampling (colours) in CESM2-WACCM. Temperatures are adjusted by the median DJF temperature bias. Boxplots are as defined in Fig. S21.
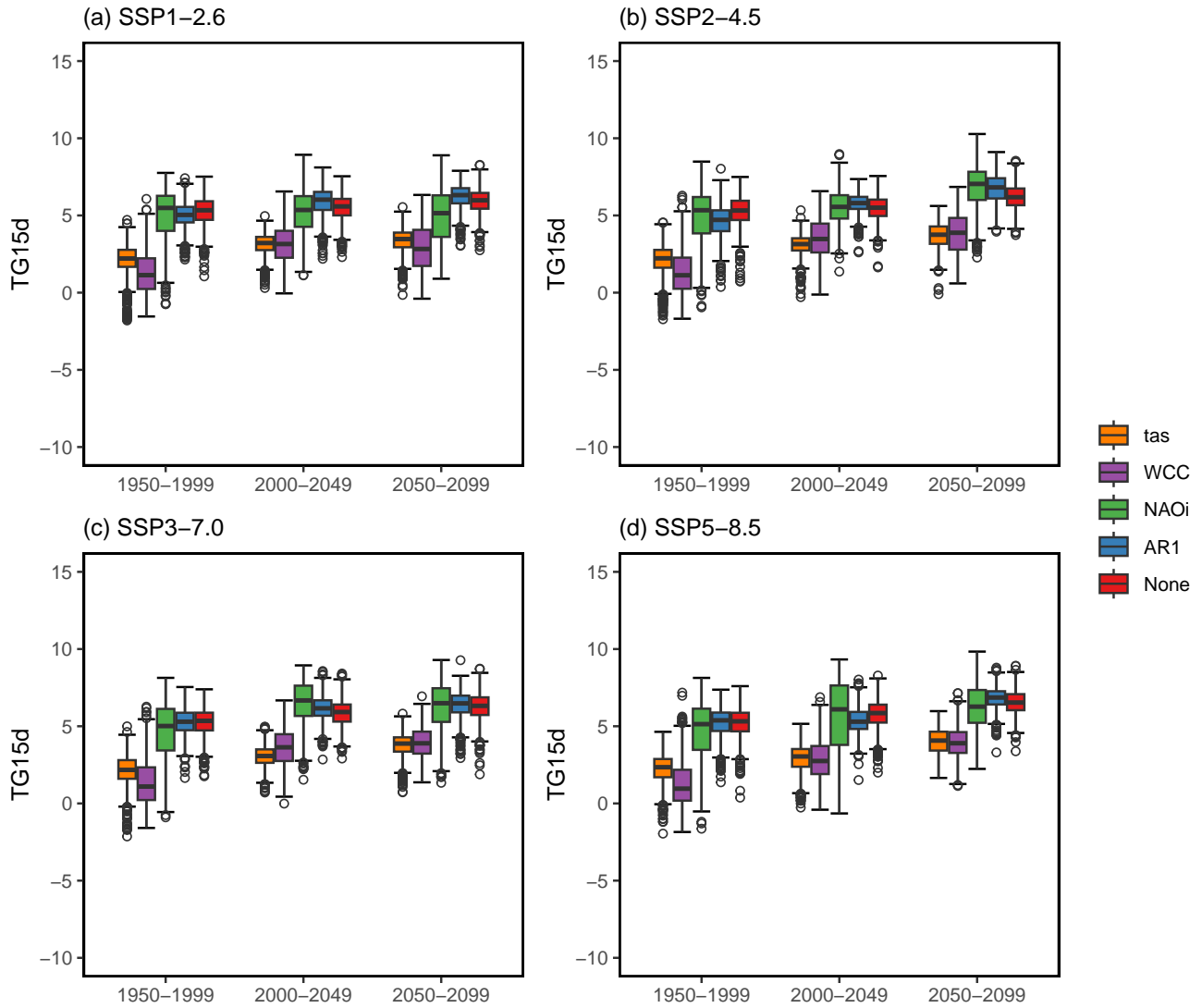
Fig. S30. Temperature (TG15d) distribution of 1000 SWG simulations for four SSPs (a-d) and three climate periods (left to right) depending on the variable used for importance sampling (colours) in NorESM2-LM. Temperatures are adjusted by the median DJF temperature bias. Boxplots are as defined in Fig. S21.